Bioorganic Chemistry 93 (2019) 103312

Contents lists available at ScienceDirect

Bioorganic Chemistry

journal homepage: www.elsevier.com/locate/bioorg

Design, synthesis, in vitro and in vivo evaluation of novel pyrrolizine-based compounds with potential activity as cholinesterase inhibitors and anti-Alzheimer's agents

Nehad Abou-Elmagd El-Sayed[a], Awatef El-Said Farag[a], Manal Abdel Fattah Ezzat[a,*], Hulya Akincioglu[b], İlhami Gülçin[c], Sahar Mahmoud Abou-Seri[a,*]

[a] Department of Pharmaceutical Chemistry, Faculty of Pharmacy, Cairo University, El-Kasr El-Eini Street, P.O. Box 11562, Cairo, Egypt
[b] Department of Chemistry, Agri Ibrahim Cecen University, Faculty of Science and Arts, 04100 Agri, Turkey
[c] Department of Chemistry, Faculty of Science, Atatürk University, 25240 Erzurum, Turkey

ARTICLE INFO

Keywords:
Alzheimer's disease
Pyrrolizine derivative
Acetylcholinesterase inhibitor
Butyrylcholinesterase inhibitor
Amyloid beta aggregation inhibition
In vivo study

ABSTRACT

Novel series of pyrrolizine based compounds (**4–6** and **9–11**) were designed, synthesized and evaluated as potential anti-Alzheimer agents. Most of the tested compounds showed selectivity to *h*AChE over *h*BChE and effectively inhibited self–induced amyloid beta aggregation in vitro. Among these derivatives, compound **10** displayed high selectivity towards *h*AChE (Ki = 1.47 ± 0.63 μM for *h*AChE and Ki = 40.15 ± 3.31 μM for *h*BChE). However, compound **11** displayed dual inhibitory effect against *h*AChE and *h*BChE at submicromolar range (Ki = 0.40 ± 0.03 and 0.129 ± 0.009 μM, respectively). Kinetic studies of the new ligands showed competitive type inhibition for both *h*AChE and *h*BChE. Moreover, compounds **10** and **11** showed lower or comparable cytotoxicity to donepezil against human neuroblastoma (SH-SY5Y) and normal human hepatic (THLE2) cell lines. In vivo studies confirmed that both compounds were able to improve cognitive dysfunction of scopolamine-induced AD mice. Finally, molecular docking simulation of compounds **10** and **11** in *h*AChE active site showed good agreement with the obtained pharmaco-biological results.

1. Introduction

Alzheimer's disease (AD) is an insidious irreversible neurodegenerative disease in the aging population [1,2]. The disease is characterized by cognitive decline with subtle problems in the executive functions [3,4]. Although it's still unknown what exactly triggers the idiopathic Alzheimer's disease but many factors are suggested to be implicated in the brain deterioration including deficiency in the neurotransmitter acetylcholine (ACh), overproduction of the amyloid-beta (Aβ) peptide, formation of neurofibrillary tangles (NFTs), disruption of metals homeostasis and formation of reactive oxygen species (ROS) [5,6]. Acetylcholine (ACh) is a neurotransmitter that is critical for particular aspects of memory tasks and alertness enhancement. Data from human studies revealed dramatic reduction of neurotransmitter ACh in the cortex and hippocampus of the afflicted brains [7]. Accordingly, the loss of cholinergic neurotransmission is the most acceptable approach in the disease etiology [8,9]. Two types of cholinesterases were identified to be responsible for ACh hydrolysis, namely acetylcholinesterase (AChE) and butyrylcholinesterase (BChE). AChE levels remains unchanged in early stages of the disease while during progression of the disease, AChE levels were found to gradually decrease and at the same time BChE remains unaltered or increased in advanced AD [10,11]. Hence, cholinergic neurotransmission can be enhanced by cholinesterase inhibitors (ChEIs) which counteract such depletion of ACh neurotransmitter and is proven to be cornerstone to alleviate AD clinical manifestations [12,13]. Currently, there are three FDA approved cholinesterase inhibitors; galantamine and donepezil are selective AChE inhibitors while rivastigmine is a dual AChE/BChE inhibitor [14]. Tacrine is another potent inhibitor of AChE and BChE that was withdrawn from market due to hepatotoxicity [15].

Furthermore, increasing evidences suggested amyloid beta (Aβ) deposition as another classic hallmark for the disease etiology [16]. Aβ is a peptide of 39 to 42 amino acids which is produced as a result of sequential proteolytic hydrolysis of amyloid precursor protein (APP) and results in formation of the senile plaques that are believed to underlie loss of cholinergic neurons and causing neuronal dysfunction in AD patients [17–19]. That's why anti-amyloidogenic agents may represent a disease modifying-treatment that will delay or bring the

* Corresponding authors.
E-mail addresses: manal.salem@pharma.cu.edu.eg (M.A.F. Ezzat), sahar.shaarawy@pharma.cu.edu.eg (S.M. Abou-Seri).

https://doi.org/10.1016/j.bioorg.2019.103312
Received 16 July 2019; Received in revised form 9 September 2019; Accepted 23 September 2019
Available online 24 September 2019
0045-2068/

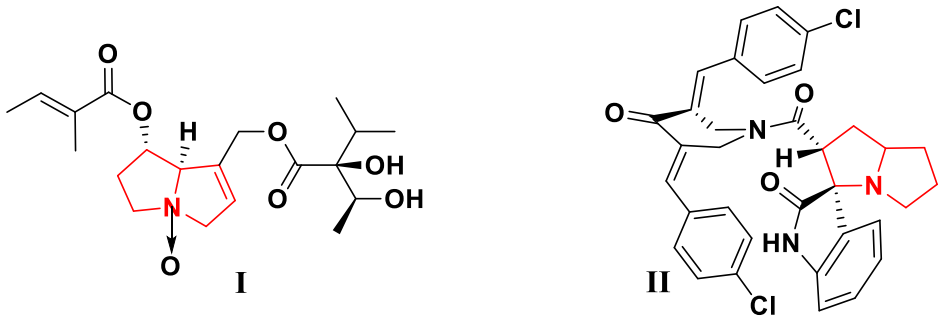

Fig. 1. Reported pyrrolizine derivatives with AChE inhibitory activity.

disease to halt contrary to current AChE inhibitors which provide only a temporary relief for AD symptoms. Therefore, ligands that can inhibit AChE activity and Aβ aggregation may result in improving the quality of life for the affected patients.

Although several heterocyclic systems have been used as a basis to discover new candidates with anti-Alzheimer's potential, yet the pyrrolizine scaffold was infrequently addressed as anti-AD agents. For example, the natural tetrahydro pyrrolizine alkaloid; 7-*O*-angeloylechinatine *N*-oxide **I**, was isolated from *Solenanthus lanatus* and showed inhibition activity against the AChE with IC_{50} 0.597 ± 0.007 mM [20]. Besides, the synthetic spirooxindole-pyrrolizine derivative **II** displayed good AChE inhibitory activity compared to galantamine (IC_{50} = 3.36 and 2.09 μM, respectively), (Fig. 1) [21,22]. At this juncture, pyrrolizine scaffold absorbed our attention to design novel donepezil-like compounds and evaluate their inhibitory effect against AChE and BChE.

The main pharmacophoric features in donepezil-like AChE inhibitors are **i)** a hydrophobic aromatic head represented by the indanone in donepezil. **ii)** Nitrogen contained midgorge binding moiety and **iii)** a terminal aryl moiety [23]. Accordingly, we herein report the design and synthesis of new series of pyrrolizine derivatives (**4a–f, 5a–f**, **6a–f** and **9–11**) which fulfill the key pharmacophoric requirements for AChE inhibition. We concentrated on three different aromatic head groups. The first series (**4a–f**) features 6-amino-2,3-dihydro-1*H*-pyrrolizine-7-carbonitrile as the main building block connected to the terminal aryl group through *N*-containing linker. The second strategy involved replacement of the carbonitrile in (**4a–f**) with carboxamide group in (**5a–f**); the carboxamide functionality is expected to stabilize the new ligands inside AChE active site through additional H-bonding interaction. In the third series (**6a–f**), the tricyclic 6,7-dihydro-3*H*-pyrimido[5,4-*a*]pyrrolizin-4(5H)-one was used. Restricting the free rotation of the carboxamide moiety of (**5a–f**) in a rigid pyrimidinone ring (**6a–f**) was envisaged to increase the chance of H- bonding interaction with AChE active site. We also checked the effect of increasing flexibility of the nitrogen containing linkers between the aromatic head group and aryl tail through the design of the phenylpiperazine derivatives versus the benzylpiperazine counterparts (**4e,f, 5e,f** and **6e,f**) together with bioisosteric replacement of the arylpiperazine moiety in series **4–6** with benzylpiperidin-4-amino motif in compounds **9–11** (Fig. 2).

The newly designed compounds were in vitro evaluated for their *h*AChE and *h*BChE inhibitory activities and the mechanism of enzyme inhibition was explored by kinetic study. The ability of compounds to inhibit the self-induced Aβ aggregation compared with curcumin was performed by ELISA. Neuroprotective effects in scopolamine-induced cognitive impairment model in mice and acute toxicity were assessed for the most active compounds. Molecular docking studies of the most potent inhibitors within *h*AChE active site were applied to explore their binding mode and justify their high affinity.

2. Results and discussion

2.1. Chemistry

The synthetic pathways employed for the preparation of target pyrrolizine derivatives is outlined in Schemes 1 and 2. Compounds **1a–f**, **2,** and **7** were synthesized according to the previously reported methods [24–27]. Next, condensation of pyrrolidin-2-ylidene malononitrile **2** with (un)substituted phenyl/benzyl-piperazin-1-yl derivatives (**1a–f**) or *N*-(1-benzylpiperidin-4-yl)-2-chloroacetamide derivative (**7**) was carried out by heating under reflux in dry acetone in the presence of potassium carbonate to obtain intermediates **3a–f** and **8**, respectively (Schemes 1 and 2). IR spectra of compounds **3a–f** and **8** revealed the presence of two CN stretching bands at 2203–2210 and 2183–2195 cm^{-1} as well as C=O stretching band vibrating at 1659–1701 cm^{-1}. Moreover, compound **8** showed an additional NH stretching band at 3364 cm^{-1}. ^{1}-HNMR spectra of these compounds demonstrated the appearance of a multiplet and two triplet signals at 1.96–2.05, 2.95–2.98 and 3.68–3.72 ppm corresponding to pyrrolidine protons in addition to a singlet signal at 4.31–4.71 ppm assigned for the CH_2 of oxoethyl spacer which confirm the success of condensation reaction. The benzyl derivatives **3e,f** and **8** showed an extra singlet signal at 3.35–3.45 ppm representing the benzylic CH_2 protons, while the amide NH proton in **8** appeared as D_2O exchangeable signal at 8.04 ppm. ^{13}C NMR spectra of compounds **3a–f** and **8** revealed the presence of two characteristic signals at 164.07–164.99 and 172.29–172.37 ppm attributed to C=O and C-2 of the pyrrolidine ring, respectively.

Intramolecular cyclization of pyrrolidin-2-ylidene malononitriles **3a–f** and **8** into the respective 6-amino-2,3-dihydro-1*H*-pyrrolizine-7-carbonitrile derivatives **4a–f** and **9** was achieved by stirring with 1% NaOEt at room temperature for 24 h (Schemes 1 and 2). IR spectra of these compounds showed the presence of only one C≡N stretching band at 2203–2222 cm^{-1} in addition to the NH_2 symmetric and asymmetric stretching bands at 3345–3449 and 3321–3356 cm^{-1}. Their ^{1}H NMR spectra revealed the disappearance of the oxoethyl signal at 4.31–4.71 ppm together with the appearance of singlet D_2O exchangeable signal at 4.91–5.31 ppm attributed to NH_2 protons. Besides, the ^{13}C- NMR spectra of compounds **4a–f** and **9** showed the presence of C=O signal resonating at 160.99–162.86.

The synthesized 6-amino-2,3-dihydro-1*H*-pyrrolizine-7-carbonitriles **4a–f** and **9** were subjected to acid catalyzed hydrolysis using 90% H_2SO_4 to yield the pyrrolizine-7-carboxamide derivatives **5a–f** and **10**, or heated under reflux with 90% formic acid to produce the tricyclic 6,7-dihydro-3*H*-pyrimido[5,4-*a*]pyrrolizin-4(5*H*)-one derivatives **6a–f** and **11** (Schemes 1 and 2).

Regarding compounds **5a–f** and **10,** the main structural features in IR spectra include the presence of multiple stretching bands related to

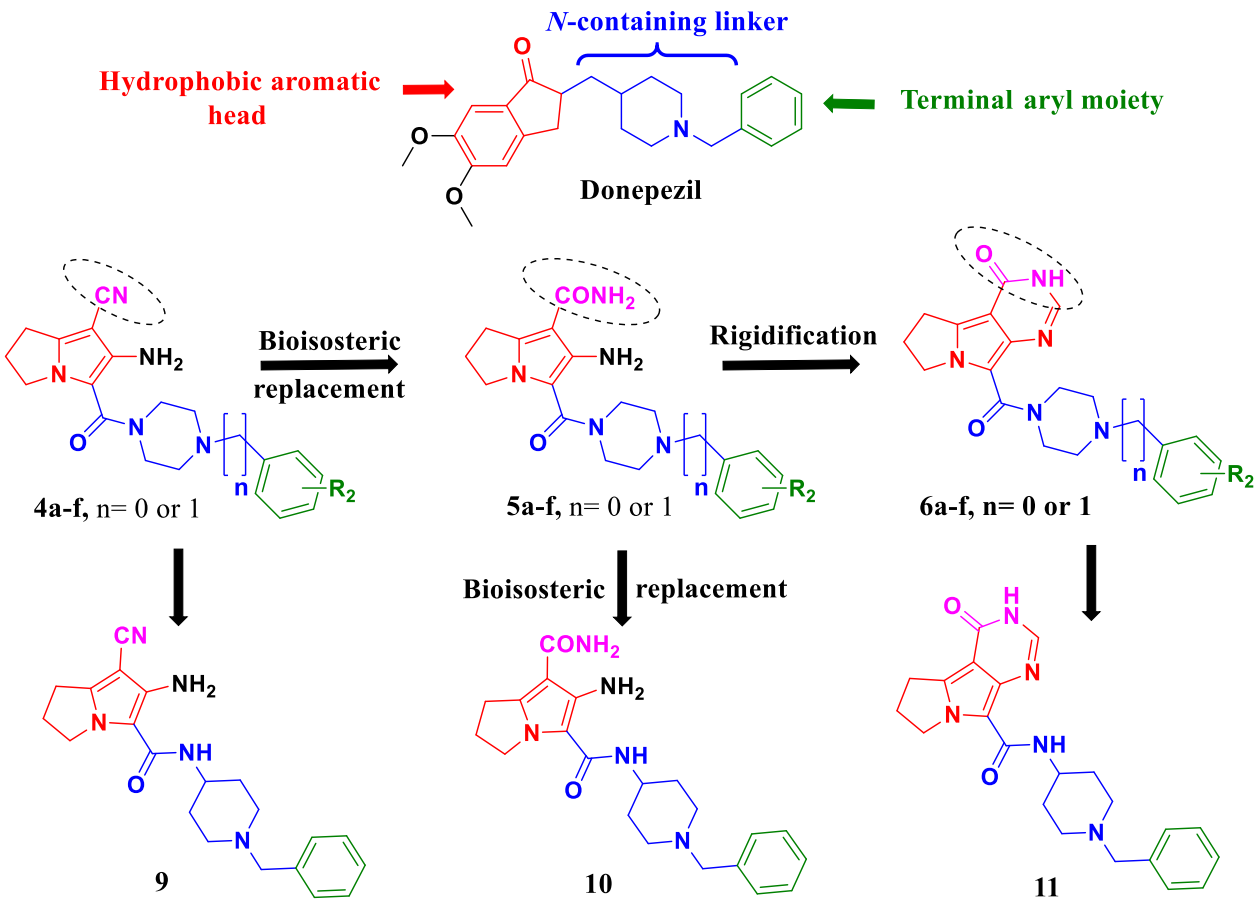

Fig. 2. Design of the target compounds.

the amino and carboxamide NH_2 groups at 3302–3534 cm^{-1} as well as two characteristic carbonyl stretching bands between 1643 and 1655 cm^{-1} beside the disappearance of the C≡N stretching band. ^{1}H NMR spectra showed the appearance of an additional singlet at 6.52–6.60 ppm attributed to carboxamide NH_2 protons which disappeared upon deuteration. ^{13}C NMR spectra of **5a–f** and **10** revealed the appearance of two characteristic signals at 161.51–164.08 and 167.17–168.19 ppm corresponding to the two C=O groups.

On the other hand, ^{1}-HNMR spectra of compounds **6a–f** and **11** showed a singlet signal at 7.70–7.86 ppm and a D_2O exchangeable singlet signal at 11.37–11.61 ppm assigned for the pyrimidinone CH and NH protons, respectively. Their ^{13}C NMR spectra revealed the appearance of two signals resonating at the range 158.52–159.01 and 160.05–161.19 ppm related to the carbons of the two carbonyl groups.

2.2. In vitro biological studies

2.2.1. Cholinesterase inhibitory activity and structure-activity relationship (SAR) study

The target compounds were evaluated for their AChE and BChE inhibitory activities by modified Elman's method [28,29] using recombinant human AChE and human serum BChE enzymes. Tacrine and donepezil were used as reference drugs. Dissociation constants for both *h*AChE and *h*BChE as well as selectivity indexes towards *h*BCh are enlisted in Table 1. The tested compounds exhibited wide range of inhibition against *h*AChE (Ki range = 0.40 ± 0.03 − > 50 μM). Meanwhile, most compounds showed fair or no inhibitory activity against *h*BChE; only compounds **6b** and **6d** inhibited *h*BChE at single digit micromolar concentrations with Ki values of 8.56 and 5.45 μM, respectively. However, compound **11** displayed dual inhibitory effect against *h*AChE and *h*BChE at submicromolar range (Ki = 0.40 ± 0.03 and 0.129 ± 0.009 μM, respectively).

Close examination of the inhibitory profile of the new compounds against *h*AChE, the following SAR can be concluded: The activity of the arylpiperazine derivatives **4–6** seems sharply dependent on the aromatic head group. The pyrrolizine-7-carbonitrile derivatives **4a–f** were found inactive (Ki > 50 μM). As expected, the activity was enhanced upon replacement of the cyano group in **4a–f** with carboxamide function in analogs **5a–f** (Ki range = 11.17 ± 3.16–22.21 ± 1.46 μM). On the same vein, the tricyclic 6,7-dihydro-3*H*-pyrimido[5,4-*a*]pyrrolizin-4(5*H*)-one derivatives **6a–f** (Ki = 6.85 ± 0.76–39.88 ± 7.85 μM) showed an increase in activity compared to their corresponding carbonitriles **4a–f**.

Regarding the impact of substituents on the terminal aryl moiety and the change of linker on the inhibitory activity of series **5a–f**; the electron-donating 4-OCH_3 substituent on the phenylpiperazine, **5d**, exhibited decreased inhibitory action (Ki = 17.36 ± 3.05 μM) relative to the unsubstituted phenylpiperazine analog **5a** (Ki = 12.15 ± 5.57 μM) or substitution with electron withdrawing groups in **5b** and **5c** (Ki = 13.32 ± 3.95 and 11.17 ± 3.16 μM, respectively). Comparing the activity of phenylpiperazine derivatives **5a–d** (Ki = 11.17 ± 3.16–17.36 ± 3.05 μM) with benzylpiperazine derivatives **5e** and **5f** (Ki = 20.11 ± 6.70 and 22.21 ± 1.46 μM, respectively) revealed that the elongation of the linker resulted in significant decrease of activity.

Conversely in series **6a–f**, the 4-OCH_3 substituted derivative **6d** exhibited the best *h*AChE inhibitory action among the phenylpiperazine derivatives **6a–d** (Ki = 10.05 ± 0.71 μM) and the order of activity was electron donating substituted > electron withdrawing substituted > unsubstituted phenyl. Moreover, linker elongation in benzyl derivatives **6e** and **6f** (Ki values = 16.58 ± 0.82 and 6.85 ± 0.76 μM, respectively) displayed a noticeable improvement of the activity rather

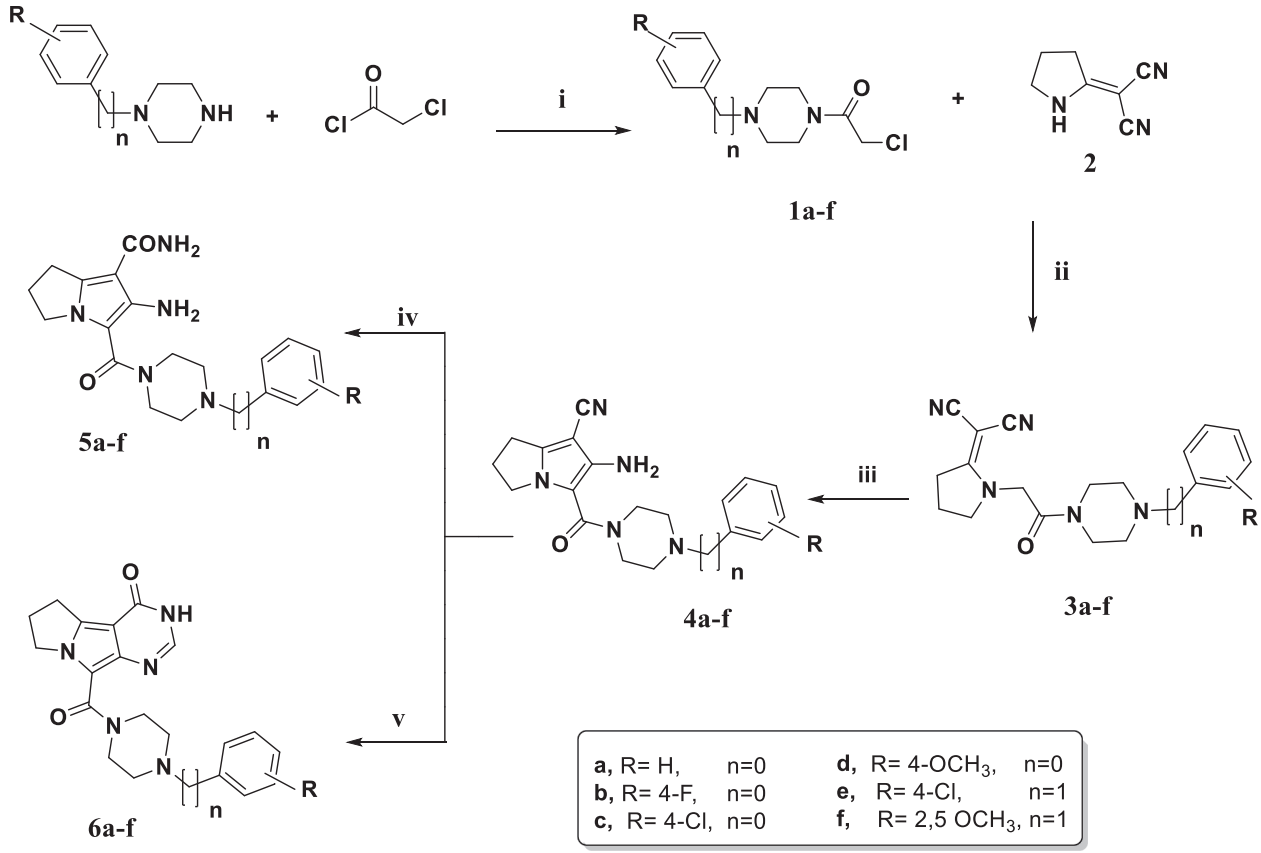

Scheme 1. Reagents and reaction conditions, **(i)**: dry benzene, 20% NaOH, 0–10 C, 3 h; **(ii)**: dry acetone, anhydrous K_2CO_3, reflux, 24 h; **(iii)**: 1% NaOEt, rt, 24 h; (iv): 90% H_2SO_4, rt, 48 h; **(v)**: 90% HCOOH, reflux, 8 h.

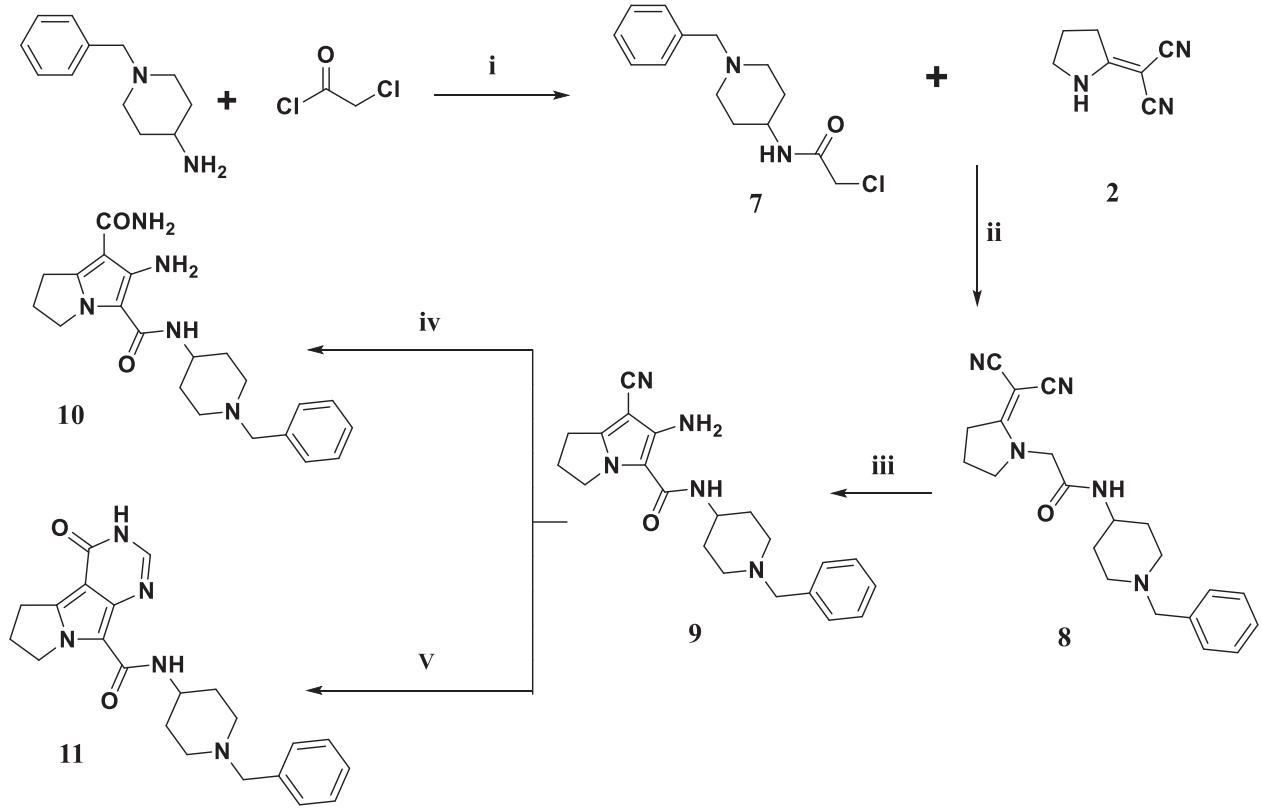

Scheme 2. Reagents and reaction conditions, **(i)**: dry benzene, 20% NaOH, 0–10 C, 3 h; **(ii)**: dry acetone, anhydrous K_2CO_3, reflux, 24 h; **(iii)**: 1% NaOEt, rt, 24 h; (iv): 90% H_2SO_4, rt, 48 h; **(v)**: 90% HCOOH, reflux, 8 h.

Table 1

Inhibition of *h*AChE, *h*BChE and self-induced $A\beta_{1-42}$ aggregation.

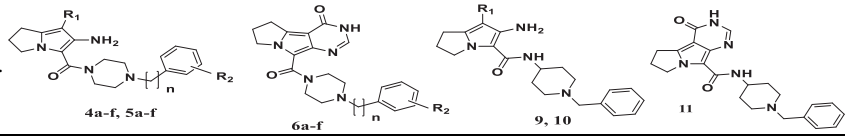

Compound	R_1	R_2	n	*h*AChE Ki (μM)[a] (IC_{50} μM)	*h*BChE Ki (μM)[a] (IC_{50} μM)	SI[b] (BChE)	Aβ inhibition IC_{50} (μM)[a]
4a	CN	H	0	> 50	> 50	–	0.65 ± 0.09
4b	CN	4-F	0	> 50	> 50	–	0.35 ± 0.09
4c	CN	4-Cl	0	> 50	> 50	–	6.11 ± 0.13
4d	CN	4-OCH_3	0	> 50	> 50	–	1.61 ± 0.10
4e	CN	4-Cl	1	> 50	> 50	–	0.25 ± 0.08
4f	CN	2,5-OCH_3	1	> 50	> 50	–	2.72 ± 0.12
5a	$CONH_2$	H	0	12.15 ± 0.87	36.51 ± 1.89	0.33	0.35 ± 0.09
5b	$CONH_2$	4-F	0	13.32 ± 0.92	> 50	< 0.27	1.47 ± 0.11
5c	$CONH_2$	4-Cl	0	11.17 ± 1.06	N.D.[c]	–	0.51 ± 0.09
5d	$CONH_2$	4-OCH_3	0	17.36 ± 1.64	28.36 ± 1.84	0.61	0.55 ± 0.09
5e	$CONH_2$	4-Cl	1	20.11 ± 0.83	> 50	< 0.40	1.97 ± 0.11
5f	$CONH_2$	2,5-OCH_3	1	22.21 ± 2.11	> 50	< 0.44	2.68 ± 0.12
6a	–	H	0	39.88 ± 2.98	41.51 ± 3.53	0.96	3.16 ± 0.12
6b	–	4-F	0	22.25 ± 1.91	8.56 ± 0.67	2.60	0.61 ± 0.09
6c	–	4-Cl	0	26.37 ± 1.88	> 50	< 0.53	1.48 ± 0.11
6d	–	4-OCH_3	0	10.05 ± 0.71	5.45 ± 0.34	1.84	0.38 ± 0.08
6e	–	4-Cl	1	16.58 ± 0.82	41.50 ± 3.92	0.40	1.80 ± 0.11
6f	–	2,5-OCH_3	1	6.85 ± 0.67	> 50	< 0.14	0.74 ± 0.09
9	CN	–	–	7.55 ± 0.63	25.74 ± 2.31	0.29	6.05 ± 0.13
10	$CONH_2$	–	–	1.47 ± 0.76 (4.17 ± 0.36)	40.15 ± 3.31 (> 50)	0.04	0.42 ± 0.09
11	–	–	–	0.40 ± 0.03 (0.73 ± 0.05)	0.129 ± 0.009 (0.74 ± 0.04)	3.10	1.67 ± 0.11
Tacrine				0.12 ± 0.01 (0.30 ± 0.02)	0.04 ± 0.0003 (0.052 ± 0.003)	3.05	
Donepezil				0.02 ± 0.001 (0.033 ± 0.002)	> 1 (0. > 1)	< 0.02	
Curcumin				–	–	–	0.63 ± 0.04

[a] Data are expressed as mean ± S.D. from three different experiments.
[b] SI (Selectivity index for BChE) which is calculated from the following equation: *h*BChE selectivity index = Ki (*h*AChE)/Ki (*h*BChE).
[c] N.D. = not determined.

than the phenyl derivatives **6a–d** (Ki = 10.05 ± 0.71–39.88 ± 7.85 μM).

Finally, the best *h*AChE inhibitory profile was observed upon a bioisosteric replacement of the arylpiperazine moiety in **4–6** with benzylpiperidin-4-amino motif in compounds **9–11.** They followed the same pattern of inhibition as the arylpiperazine derivatives with respect to the effect of the aromatic head groups. The pyrrolizin-7-carbonitrile derivative **9** was found the least active among benzylpiperidines (Ki = 7.55 ± 1.87 μM). Replacement of the pyrrolizin-7-carbonitrile head in **9** with pyrrolizidin-7-carboxamide in **10** (Ki = 1.47 ± 0.63 μM) or 6,7-dihydro-3*H*-pyrimido[5,4-*a*]pyrrolizin-4(5*H*)-one in **11** (Ki = 0.40 ± 0.05 μM) resulted in the most potent *h*AChE inhibitors in this study with 5 and 18 fold increase in potency, respectively.

Analysis of the selectivity of the synthesized molecules revealed that, most compounds are less selective to *h*BChE (SI = 0.04 – 2.60). Compound **10** was the least selective to *h*BChE (SI = 0.04), meanwhile compound **11** was a potent dual inhibitor of *h*AChE and *h*BChE (SI = 3.10). Despite the fact that BChE activity is lower than that of *h*AChE in the normal brain and early stages of AD, the BChE/AChE ratio is greatly increased in advanced AD, which suggests that inhibition of BChE may become more important as AD progresses. This raises the hypothesis that inhibitory action on both ChEs leads to improved therapeutic benefits. Accordingly, compound **11** which act as a dual *h*AChE/*h*BChE inhibitor may serve as a good lead for further optimization to relief the disease symptoms in moderate to advanced AD stages. On the contrary, compound **10** with good selectivity towards *h*AChE can be considered for further study to discover new candidates for management of early stages AD symptoms.

Finally, the IC_{50} values were calculated for the most promising compounds, **10** (IC_{50} = 4.17 ± 0.36 μM) and **11** (IC_{50} = 0.74 ± 0.05). The results revealed that both compounds showed comparable inhibition profile to the reference tacrine (IC_{50} = 0.30 ± 0.02 μM), however both compounds still less potent (20 folds or more) than the reference drug donepezil (IC_{50} = 0.033 ± 0.002 μM).

2.2.2. Kinetic studies of synthesized molecules

Kinetic study was performed to elucidate the interaction mechanism of the target compounds with *h*AChE and *h*BChE. The study was performed following the modified Ellman's method [28,29]. The Lineweaver-Burk reciprocal plots (1/V *vs* 1/S) were analyzed and unveiled that all compounds possess diverse slopes and intercepts on x-axis and the same intercept on the y-axis at increasing concentration of the inhibitors (Fig. 3). This pattern is consistent with competitive inhibition of the synthesized compounds on both *h*AChE and *h*BChE.

2.2.3. Self-induced amyloid-beta aggregation

One of the distinct markers of AD is the extracellular aggregation of fibrous protein deposits called amyloid plaques, which is considered as one of the critical causes that accelerate consequent events and trigger the progression of Alzheimer's disease (AD). Amyloid beta (Aβ) is the main component of the amyloid plaques and a distinct morphological feature found in the Alzheimer's brains. Accordingly, blocking Aβ aggregation is an alternative approach to control AD [17–19].

Aβ has two isoforms, $A\beta_{1-42}$ and $A\beta_{1-40}$ but $A\beta_{1-42}$ is of lower solubility and higher neuronal toxicity than $A\beta_{1-40}$ [19]. Therefore, the ability of the synthesized compounds to inhibit the self-induced $A\beta_{1-42}$

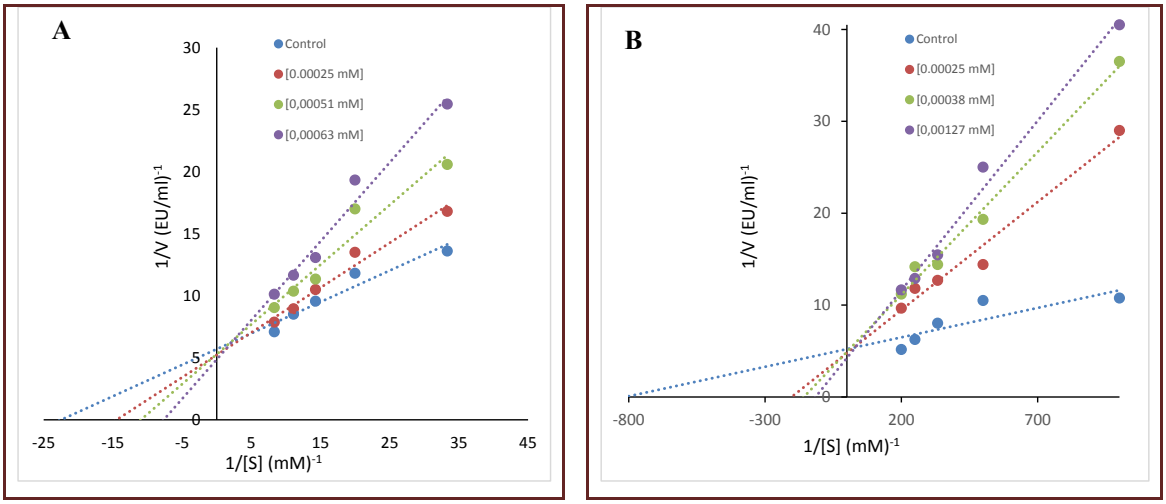

Fig. 3. Lineweaver-Burk plot for inhibition of *h*AChE **(A)** and *h*BChE **(B)** by compound **11.**

aggregation was assessed by enzyme-linked immunosorbent assay (ELISA) method [30]. Curcumin, a known active natural product for inhibition of $A\beta_{1-42}$ self-aggregation, was employed as reference compound. Results are listed in Table 1 and summarized in Fig. 4. The tested compounds displayed moderate to high inhibitory effect on Aβ aggregation compared to curcumin (IC_{50} = 0.63 ± 0.04 μM). Compounds **4b, 4e, 5a, 6d** and **10** showed significantly better inhibitory effect than curcumin with IC_{50} values ranging from 0.25 ± 0.08 to 0.42 ± 0.09 μM, while compounds **4a, 5c, 5d, 6b** and **6f** were almost equipotent to the reference compound (IC_{50} = 0.51 ± 0.09–0.65 ± 0.09 μM). Moreover, compounds **4d**, **5b**, **5e**, **6c, 6e** and **11** exhibited comparable activity to curcumin with IC_{50} range = 1.47 ± 0.11–1.97 ± 0.11 μM. These results suggested pyrrolizine as a promising new scaffold that may exert neuroprotective activity toward Aβ-induced toxicity.

*2.2.4. Toxicity of the compound **10** and **11**on SH-SY5Y cell and THLE2 cells*

Given the fact that, compound **11** with the most potent AChE/BChE inhibitory activity and compound **10** with highest selectivity towards AChE efficiently inhibited the self-mediated $A\beta_{1-42}$ aggregation; they were selected to be advanced for further in vivo studies. Before moving to in vivo testing, the safety of compounds **10** and **11** was evaluated by investigating their cytotoxicity against human neuroblastoma (SH-SY5Y) and normal human hepatic (THLE2) cell lines using a 3-(4,5-dimethylthiazol-2-yl)-2,5-diphenyltetrazolium bromide (MTT) assay [31]. As shown in Fig. 5, compounds **10** and **11** exhibited comparable or lower cytotoxicity on both cell lines when compared to the clinically used drug, donepezil.

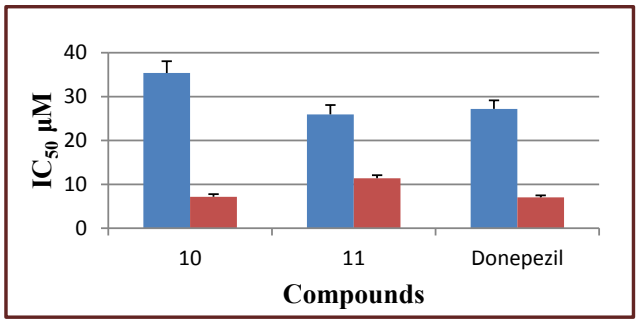

Fig. 5. The cytotoxic effects of compounds **10, 11** and donepezil on THLE2 (blue) and SH-SY5Y (red) human cell lines. Results are expressed as IC_{50} (μM) ± SD.

2.3. In vivo behavioral studies

Compounds **10** and **11** showed the best results in in vitro AChE studies in addition to superior or comparable activity to curcumin as anti-amyloidogenic agents and low toxicity toward hepatic and neuronal cell lines, therefore they were evaluated for their ability to ameliorate impaired learning and memory functions in vivo. Memory impairment was induced by administering scopolamine then Y-maze test [32] and step-through passive avoidance test [33] were performed. Donepezil was used as positive control.

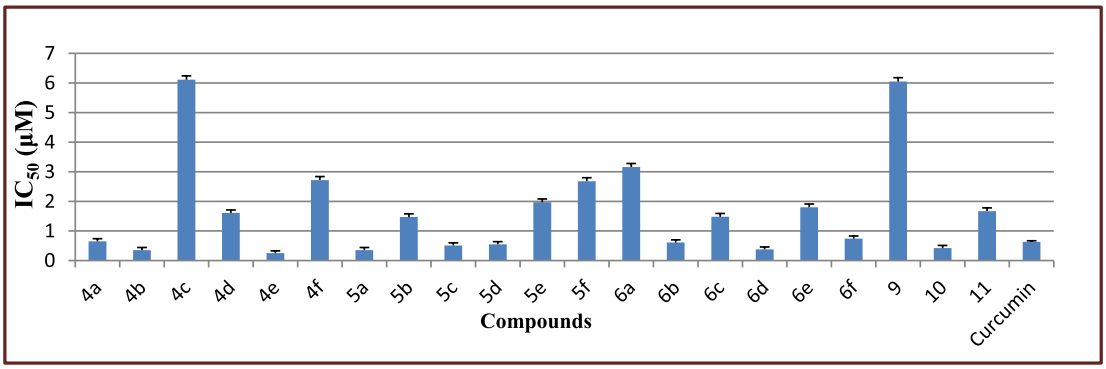

Fig. 4. Inhibition of self-induced $A\beta_{1-42}$ aggregation by the newly synthesized compounds comparing with that of curcumin. The mean ± SD values from three independent experiments were shown.

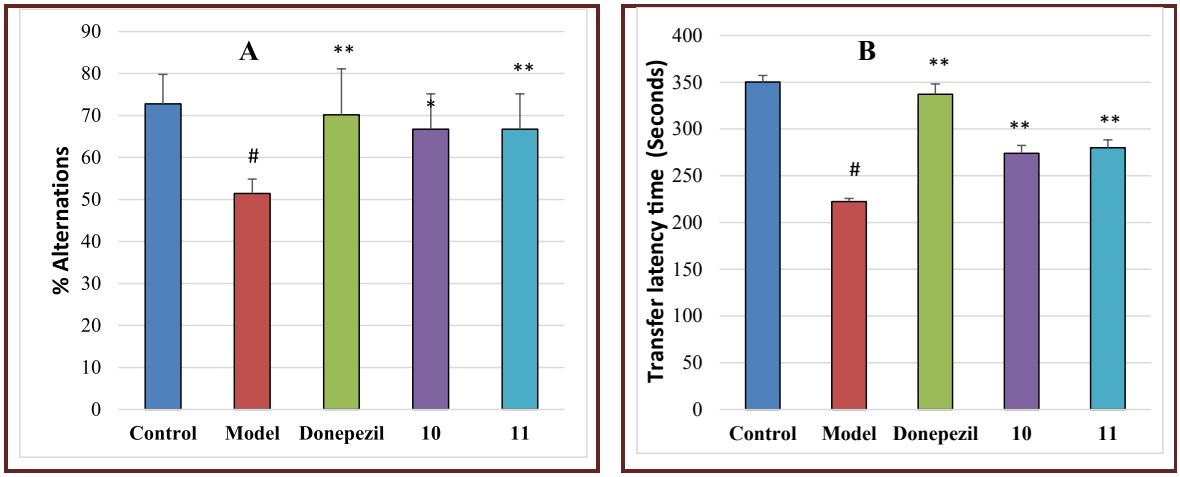

Fig. 6. (A) % of spontaneous alternations in the Y-maze test. (**B**) The transfer latency time in seconds for step-through passive avoidance test. Data are presented as mean ± S.D. (n = 5; #p < 0.01 *vs* control group, and *p < 0.05, **p < 0.01 *vs* model group).

In Y-maze test (Fig. 6A), the scopolamine model group exhibited lower percentage of alternations than the control group (% alternations = 51.42 and 72.30, respectively, at #p < 0.01). Mice groups treated with compounds **10** and **11** showed a significant increase in the percentage of alternations compared to the model group [% alternations = 61.80 (*p < 0.05) and 66.70 (**p < 0.01) respectively].

We also measured the defending effect of compounds **10** and **11** against memory deficit using the step-through passive avoidance test. The transfer latency time (TLT) was measured and illustrated in Fig. 6B. In comparison with the control, the TLT of scopolamine treated group (TLT = 222.4 s, at #p < 0.01) was significantly reduced than that of the control (TLT = 350.2 s). Meanwhile, treatment with compounds **10** (TLT = 276 s) or **11** (TLT = 280 s) reversed the scopolamine lowered TLT compared to the model group (**p < 0.01). These results demonstrated that compounds **10** and **11** were able to pass the blood brain barrier and improve scopolamine induced cognitive deficit.

2.4. Molecular docking studies

In order to explore the possible binding mode of compounds **10** and **11** within AChE active site and justify their potency, a molecular docking study was conducted using Molecular Operating Environment software (MOE 2008.10) [34]. The X-ray crystallographic structure of recombinant human AChE (r*h*AChE) in complex with donepezil (PDB code **4EY7**) was obtained from the Protein Data Bank. The AChE active site consists mainly of three subsites; a peripheral anionic site (PAS) including Trp286, Tyr124, Asp74 and Phe295, a mid-aromatic gorge and a catalytic active site (CAS) composed of Trp86, Glu202, Tyr337 and Gly448 residues [35]. Inspection of the top docking poses of compound **10** and **11** showed that, the pyrrolizine head in both compounds is engaged in an important π-π stacking with aromatic residue of Trp86 in CAS. Also, H-bond interaction was observed between carboxamide NH_2 in compound **10** or the pyrimidinone NH in compound **11** and Glu202 in the CAS. This H-bond may play an important role in stabilization of the ligands inside the CAS and supported our hypothesis that the incorporation of an amide fragment to pyrrolizine head may be beneficial to enhance the binding and improve the AChE inhibitory activity. Moreover, compound **10** formed an H-bond interaction with Tyr124 through the amide carbonyl group in the linker, whereas the amide carbonyl group in compound **11** displayed water mediated H-bond with Tyr337 and Tyr341. The protonated nitrogen atom of the piperidine ring in both compounds bind to Tyr341 via a cation-π interaction as well as H-bond interaction with Tyr124, while the benzyl moiety was involved in π-π interaction with Trp286 (Fig. 7).

3. Conclusion

New series of pyrrolizine derivatives were designed and synthesized as potential anti-Alzheimer agents. The compounds were evaluated for their *h*AChE and *h*BChE inhibitory activities. The results indicated that compounds **10** and **11** possessed the highest *h*AChE inhibitory effect. Compound **10** showed good selectivity to *h*AChE over *h*BChE (Ki = 1.47 ± 0.63 μM for AChE and Ki = 40.15 ± 3.31 μM for BChE), while compound **11** displayed dual inhibitory effect on *h*AChE/*h*BChE (Ki = 0.40 ± 0.03 and 0.129 ± 0.009 μM, respectively). SAR study, supported by molecular docking, revealed that *h*AChE inhibitory activity is enhanced by grafting of an amide fragment to the pyrrolizine head as well as introduction of *N*-(1-benzylpiperidin-4-yl)acetamide moiety. Moreover, compounds **10** and **11** effectively inhibited Aβ aggregation and exhibited low toxicity on THLE2 and SH-SY5Y cell lines in vitro. Finally, both compounds significantly improved the cognition impairment in scopolamine treated mice in Y maze and step-through passive avoidance tests. Therefore, compounds **10** and **11** could be considered as good lead candidates for further optimization and development of more potent anti-Alzheimer's agents.

4. Experimental section

4.1. Chemistry

4.1.1. General

All chemicals and solvents were purchased from commercial suppliers and were used without further purification. Melting points were taken on a Electrothermal 9100 melting point apparatus. The IR spectra (KBr discs) were obtained on a Schimadzu FT-IR 8400S spectrophotometer (Kyoto, Japan) and expressed in wave number (cm^{-1}). ^{1}H NMR spectra were recorded on a Bruker Ascend 400 MHz spectrometer and ^{13}C NMR spectra were recorded at 100 MHz in deuterated (DMSO-d_6). Chemical shift values (δ) are expressed as parts per million (ppm). All coupling constant (J) values are given in hertz. TLC was performed using silica gel plates containing UV indicator to follow the course of reactions and to ensure the purity of products, using chloroform: methanol 8.5: 1.5 as the eluting system. The elemental analysis was carried out at the Mycology and Biotechnology center, Al-Azhar University. **1a–f**, **2,** and **7** were synthesized according to the previously reported methods [24–27].

4.1.2. General synthetic procedure for *3a–f* and *8*

A mixture of compound **2** (1gm, 7.5 mmol), compounds **1a–f** or **7** (7.5 mmol) and powdered anhydrous potassium carbonate (2.1 gm,

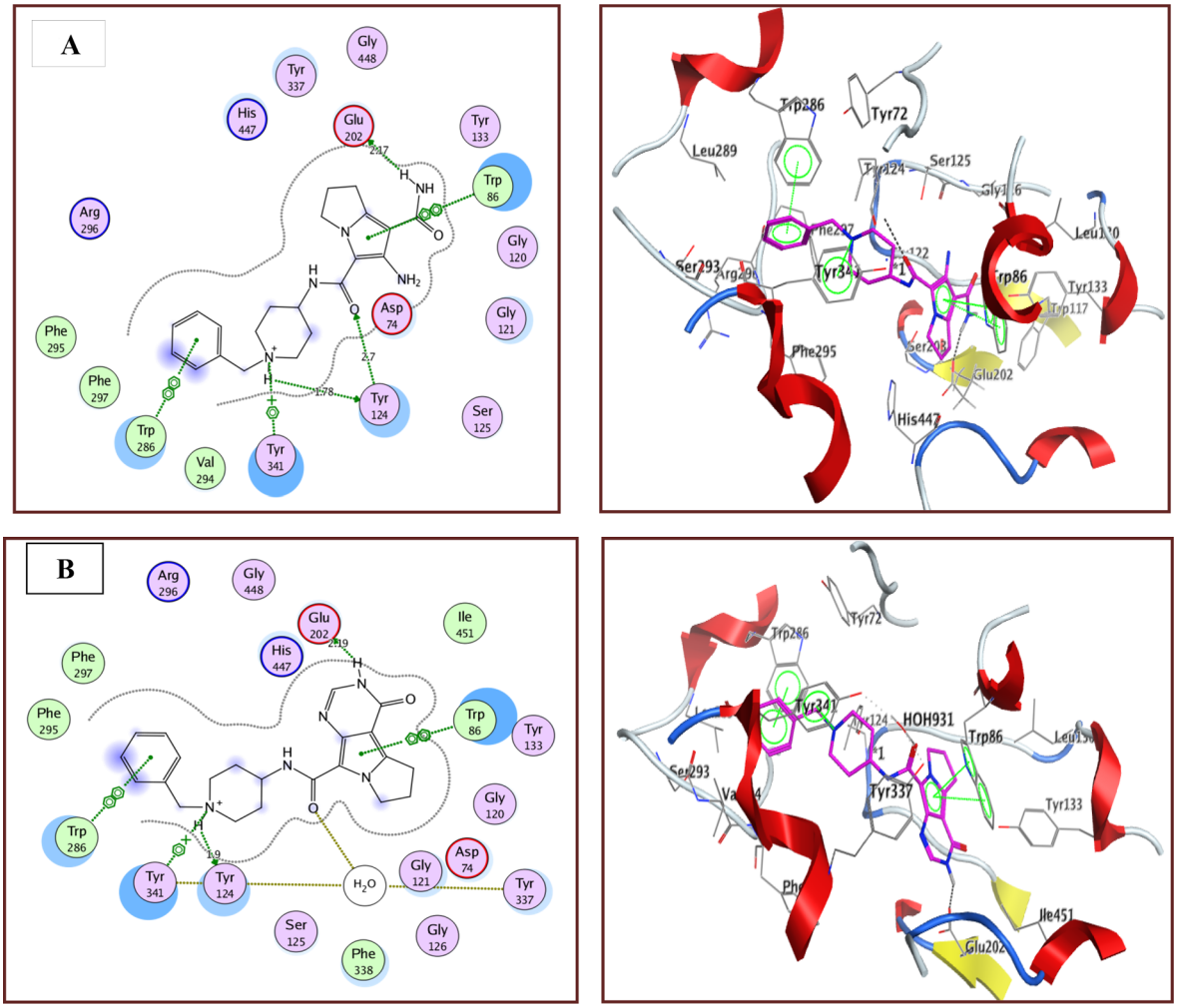

Fig. 7. 2D and 3D style presentation of the binding interactions between the most active compounds **10 (A)** and compound **11 (B)** with *rh*AChE active site.

15 mmol) in dry acetone (30 mL) was refluxed for 8 h then filtered while hot. The filtrate was concentrated and set aside to cool. The formed white crystals were collected, washed with ethanol, dried and recrystallized from ethanol to afford the corresponding intermediates **3a–f** and **8**, respectively.

*4.1.2.1. 2-{1-[2-Oxo-2-(4-phenylpiperazin-1-yl)ethyl]pyrrolidin-2-ylidene}malononitrile(**3a**).* Yield: 91%; m.p.: 160–162 °C; IR (υ_{max}, cm^{-1}): 3067 (CH-Ar.), 2967 (CH aliph.), 2203 and 2187 (2C≡N), 1663 (C=O); ^{1}H NMR (DMSO-d_6, 400 MHz): δ 1.99–2.03 (m, 2H, CH_2 of pyrrolidine), 2.98 (t, 2H, CH_2 of pyrrolidine, J = 7.84 Hz), 3.14 (t, 2H, CH_2 of piperazine, J = 4.86 Hz), 3.2 (t, 2H, CH_2 of piperazine, J = 4.76 Hz), 3.51 (t, 2H, CH_2 of piperazine, J = 4.64 Hz), 3.62 (t, 2H, CH_2 of piperazine, J = 4.80 Hz), 3.71 (t, 2H, CH_2 of pyrrolidine, J = 7.24 Hz), 4.71 (s, 2H, N−C$\underline{H_2}$C=O), 6.82 (t, 1H, Ar-H, J = 7.24 Hz), 6.96 (d, 2H, Ar-Hs, J = 8.00 Hz), 7.25 (t, 2H, Ar-Hs, J = 7.4 Hz); ^{13}C NMR (DMSO-d_6, 100 MHz): δ 19.69, 36.28, 42.04, 43.42, 44.29, 48.37, 48.65, 49.42, 59.55, 116.35, 116.53 118.13, 119.85, 129.48, 151.17, 164.25 (C=O), 172.36 ($\underline{C}$=C-2C≡N); Anal. Calcd for $C_{19}H_{21}N_5O$: C, 68.04; H, 6.31; N, 20.88. Found: C, 67.89; H, 6.45; N, 21.14.

*4.1.2.2. 2-{1-(2-[4-(4-Fluorophenyl)piperazin-1-yl]-2-oxoethyl) pyrrolidin-2-ylidene}malononitrile(**3b**).* Yield: 90%; m.p.: 165–167 °C; IR (υ_{max}, cm^{-1}): 3066 (CH-Ar.), 2835 (CH aliph.), 2203 and 2191 (2C≡N), 1667 (C=O); ^{1}H NMR (DMSO-d_6, 400 MHz): δ 1.98–2.05 (m, 2H, CH_2 of pyrrolidine), 2.98 (t, 2H, CH_2 of pyrrolidine, J = 7.80 Hz), 3.08 (s, br., 2H, CH_2 of piperazine), 3.14 (s, br., 2H, CH_2 of piperazine), 3.51 (s, br., 2H, CH_2 of piperazine), 3.62 (s, br., 2H, CH_2 of piperazine), 3.71 (t, 2H, CH_2 of pyrrolidine, J = 7.22 Hz), 4.71 (s, 2H, N−C$\underline{H_2}$C=O), 6.96–6.70 (dd, 2H, Ar-Hs, $^4J_{F\text{-}H}$ = 4.62 Hz and 9.02 Hz), 7.07 (t, 2H, Ar-Hs, $^3J_{F\text{-}H}$ = 8.60 Hz); ^{13}C NMR (DMSO-d_6, 100 MHz): δ 19.68, 36.28, 42.06, 43.41, 44.32, 49.15, 49.42, 49.47, 59.55, 115.84 ($^2J_{F\text{-}C}$ = 22.00 Hz), 116.52, 118.12, 118.24 ($^3J_{F\text{-}C}$ = 8.00 Hz), 148.07, 156.78($^1J_{F\text{-}C}$ = 235.00 Hz), 164.25 (C=O), 172.37 ($\underline{C}$=C-2C≡N); Anal. Calcd for $C_{19}H_{20}FN_5O$: C, 64.58; H, 5.70; N, 19.82. Found: C, 64.90; H, 5.87; N, 20.09.

*4.1.2.3. 2-{1-(2-[4-(4-Chlorophenyl)piperazin-1-yl]-2-oxoethyl)pyrrolidin-2-ylidene}malononitrile(**3c**).* Yield: 93%; m.p.: 166–168 °C; IR (υ_{max}, cm^{-1}): 3072 (CH-Ar.), 2916 (CH aliph.), 2203 and 2187 (2C≡N), 1667 (C=O); ^{1}H NMR (DMSO-d_6, 400 MHz): δ 1.99–2.03 (m, 2H, CH_2 of pyrrolidine), 2.98 (t, 2H, CH_2 of pyrrolidine, J = 7.82 Hz), 3.14 (s, br., 2H, CH_2 of piperazine), 3.2 (s, br., 2H, CH_2 of piperazine), 3.50 (s, br., 2H, CH_2 of piperazine), 3.61 (s, br., 2H, CH_2 of piperazine), 3.71 (t, 2H, CH_2 of pyrrolidine, J = 7.22 Hz), 4.71 (s, 2H, N−C$\underline{H_2}$C=O), 6.97 (d, 2H, Ar-Hs, J = 8.96 Hz), 7.26 (d, 2H, Ar-Hs, J = 8.88 Hz); ^{13}C NMR (DMSO-d_6, 100 MHz): δ 19.69, 36.28, 42.04, 43.42, 44.29, 48.37, 48.65, 49.42, 59.55, 116.35, 116.52, 118.13, 119.85, 129.48, 151.17, 164.24 (C=O), 172.36 ($\underline{C}$=C-2C≡N); Anal. Calcd for $C_{19}H_{20}ClN_5O$: C, 61.70; H, 5.45; N, 18.94. Found: C, 61.86; H, 5.63; N, 19.21.

*4.1.2.4. 2-{1-(2-[4-(4-Methoxyphenyl)piperazin-1-yl]-2-oxoethyl) pyrrolidin-2-ylidene}malononitrile(**3d**).* Yield: 84%; m.p.: 170–172 °C; IR

(υ_{max}, cm^{-1}): 3065 (CH-Ar.), 2920 (CH aliph.), 2203 and 2183 (2C≡N), 1659 (C=O); ^{1}H NMR (DMSO-d_6, 400 MHz): δ 1.98–2.05 (m, 2H, CH_2 of pyrrolidine), 2.96–3.00 (m, 4H, CH_2 of pyrrolidine and CH_2 of piperazine), 3.06 (t, 2H, 1CH_2 of piperazine, J = 4.40 Hz), 3.49 (t, 2H, CH_2 of piperazine, J = 4.72 Hz), 3.61 (t, 2H, CH_2 of piperazine, J = 4.64 Hz), 3.69 (s, 3H, OCH_3), 3.72 (t, 2H, CH_2 of pyrrolidine, J = 7.20 Hz), 4.70 (s, 2H, N−C$\underline{H_2}$C=O), 6.84 (d, 2H, Ar-Hs, J = 9.08 Hz), 6.92 (d, 2H, Ar-Hs, J = 9.08 Hz); ^{13}C NMR (DMSO-d_6, 100 MHz): δ 19.68, 36.28, 42.21, 43.41, 44.46, 49.41, 49.84, 50.16, 55.65 (OCH_3), 59.54, 114.77, 116.51, 118.14, 118.52, 145.52, 153.81, 164.19 (C=O), 172.35 ($\underline{C}$=C-2C≡N); Anal. Calcd for $C_{20}H_{23}N_5O_2$: C, 65.73; H, 6.34; N, 19.16 Found: C, 65.90; H, 6.45; N, 19.43.

*4.1.2.5. 2-{1-(2-[4-(4-Chlorobenzyl)piperazin-1-yl]-2-oxoethyl) pyrrolidin-2-ylidene}malononitrile(**3e**).* Yield: 74%; yellow oil; IR (υ_{max}, cm^{-1}): 3040 (CH-Ar.), 2947 (CH aliph.), 2203 and 2187 (2C≡N), 1670 (C=O); ^{1}H NMR (DMSO-d_6, 400 MHz): δ 1.98–2.02 (m, 2H, CH_2 of pyrrolidine), 2.37 (s, br., 2H, CH_2 of piperazine), 2.40 (s, br., 2H, CH_2 of piperazine), 2.97 (t, 2H, CH_2 of pyrrolidine, J = 7.82 Hz), 3.35 (s, 2H, benzylic CH_2), 3.47 (s, br., 4H, CH_2 of piperazine), 3.68 (t, 2H, CH_2 of pyrrolidine, J = 7.36 Hz), 4.64 (s, 2H, N−C$\underline{H_2}$C=O), 7.34 (d, 2H, Ar-Hs, J = 8.40 Hz), 7.39 (d, 2H, Ar-Hs, J = 8.40 Hz); ^{13}C NMR (DMSO-d_6, 100 MHz): δ 19.67, 36.27, 42.23, 43.39, 44.41, 49.36, 52.19, 52.51, 59.50, 61.30 (benzylic CH_2), 116.44, 118.13, 128.65, 131.05, 132.00, 137.45, 164.11 (C=O), 172.29 ($\underline{C}$=C-2C≡N); Anal. Calcd for $C_{20}H_{22}ClN_5O$: C, 62.58; H, 5.78; N, 18.24. Found: C, 62.71; H, 5.99; N, 18.47.

*4.1.2.6. 2-{1-(2-[4-(2,5-Dimethoxybenzyl)piperazin-1-yl]-2-oxoethyl) pyrrolidin-2-ylidene}malononitrile(**3f**).* Yield: 68%; yellow oil; IR (υ_{max}, cm^{-1}): 3009 (CH-Ar.), 2963 (CH aliph.), 2207 and 2187 (2C≡N), 1669 (C=O); ^{1}H NMR (DMSO-d_6, 400 MHz): δ 1.98–2.01 (m, 2H, CH_2 of pyrrolidine), 2.38–2.39 (m, 4H, CH_2 of piperazine), 2.96 (t, 2H, CH_2 of pyrrolidine, J = 7.81 Hz), 3.39 (s, 2H, benzylic CH_2), 3.46 (s, br., 4H, CH_2 of piperazine), 3.70 (s, 5H, CH_2 of pyrrolidine and OCH_3), 3.72 (s, 3H, OCH_3), 4.63 (s, 2H, N−C$\underline{H_2}$C=O), 6.78–6.81 (m, 1H, Ar-H), 6.89–6.91 (m, 2H, Ar-Hs); ^{13}C NMR (DMSO-d_6, 100 MHz): δ 19.65, 36.27, 42.30, 43.36, 44.47, 49.34, 50.11, 52.68, 55.72 (OCH_3), 56.34 (OCH_3), 59.50, 59.92 (benzylic CH_2), 112.36, 112.63, 116.27, 118.15, 127.09, 151.97, 153.50, 164.07 (C=O), 172.29 ($\underline{C}$=C-2C≡N); Anal. Calcd for $C_{22}H_{27}N_5O_3$: C, 64.53; H, 6.65; N, 17.10. Found: C, 64.67; H, 6.89; N, 17.27.

*4.1.2.7. N-(1-Benzylpiperidin-4-yl)-2-[2-(dicyanomethylene) Pyrrolidin-1-yl]acetamide(**8**).* Yield: 68%; m.p.: 159–161 °C; IR (υ_{max}, cm^{-1}): 3364 (NH), 3065 (CH-Ar.), 2928 (CH aliph.), 2210 and 2195 (2C≡N), 1701 (C=O); ^{1}H NMR (DMSO-d_6, 400 MHz): δ 1.37–1.44 (m, 2H, CH_2 of piperidine), 1.72–1.74 (m, 2H, CH_2 of piperidine), 1.96–2.04 (m, 4H, CH_2 of piperidine and CH_2 of pyrrolidine), 2.72–2.75 (m, 2H, CH_2 of piperidine), 2.95 (t, 2H, CH_2 of pyrrolidine, J = 7.76 Hz), 3.45 (s , 2H, benzylic CH_2), 3.57–3.58 (m, 1H, CH of piperidine), 3.69 (t, 2H, CH_2 of pyrrolidine, J = 7.18 Hz), 4.31 (s, 2H, N−C$\underline{H_2}$C=O), 7.24–7.34 (m, 5H, Ar-Hs), 8.04 (d, 1H, NH exchanged with D_2O); ^{13}C NMR (DMSO-d_6, 100 MHz): δ 19.62, 21.57, 31.57, 33.82, 36.40, 43.33, 50.04, 50.11, 52.07, 59.38, 62.31 (benzylic CH_2), 116.16, 116.31, 118.27, 127.51, 128.66, 129.34, 164.99 (C=O), 172.30 ($\underline{C}$=C-2C≡N); Anal. Calcd for $C_{21}H_{25}N_5O$: C, 69.40; H, 6.93; N, 19.27. Found: C, 69.73; H, 6.85; N, 19.51.

*4.1.3. General synthetic procedure for **4a–f** and **9***

Compounds **3a–f** or **8** (4.5 mmol) were treated with 1% $NaOC_2H_5$ (30 mL), allowed to stir at room temperature for 24 h. The obtained crystals were collected, washed with ethanol, dried and recrystallized from ethanol to obtain the targeted compounds **4a–f** and **9**, respectively.

*4.1.3.1. 6-Amino-5-(4-phenylpiperazine-1-carbonyl)-2,3-dihydro-1H-pyrrolizine-7-carbonitrile(**4a**).* Yield: 78%; m.p.: 219–221 °C; IR (υ_{max}, cm^{-1}): 3391 and 3333 (NH_2), 3032 (CH-Ar.), 2978 (CH aliph.), 2222 (C≡N), 1643 (C=O); ^{1}H NMR (DMSO-d_6, 400 MHz): δ 2.36–2.40 (m, 2H, CH_2 of pyrrolizine), 2.87 (t, 2H, CH_2 of pyrrolizine, J = 7.38 Hz), 3.17 (t, 4H, CH_2 of piperazine, J = 4.74 Hz), 3.57 (t, 4H, CH_2 of piperazine, J = 4.9 Hz), 3.98 (t, 2H, CH_2 of pyrrolizine, J = 7.10 Hz), 5.00 (s, 2H, NH_2 exchanged with D_2O), 6.81 (t, 1H, Ar-H, J = 7.24 Hz), 6.97 (d, 2H, Ar-Hs, J = 7.92 Hz), 7.23 (t, 2H, Ar-Hs, J = 7.34 Hz); ^{13}C NMR (DMSO-d_6, 100 MHz): δ 24.96, 25.32, 45.07, 48.51, 49.05, 75.25, 106.12, 116.31, 119.67, 129.44, 141.73, 145.90, 151.38, 162.86 (C=O); Anal. Calcd for $C_{19}H_{21}N_5O$: C, 68.04; H, 6.31; N, 20.88. Found: C, 68.04; H, 6.48; N, 21.09.

*4.1.3.2. 6-Amino-5-[4-(4-fluorophenyl)piperazine-1-carbonyl]-2,3-dihydro-1H-pyrrolizine-7-carbonitrile(**4b**).* Yield: 85%; m.p.: 227–229 °C; IR (υ_{max}, cm^{-1}): 3387 and 3333 (NH_2), 3051 (CH-Ar.), 2940 (CH aliph.), 2222 (C≡N), 1643 (C=O); ^{1}H NMR (DMSO-d_6, 400 MHz): δ 2.36–2.40 (m, 2H, CH_2 of pyrrolizine), 2.87 (t, 2H, CH_2 of pyrrolizine, J = 7.38 Hz), 3.11 (t, 4H, CH_2 of piperazine, J = 4.56 Hz), 3.56 (t, 4H, CH_2 of piperazine, J = 4.82 Hz), 3.97 (t, 2H, CH_2 of pyrrolizine, J = 7.08 Hz), 5.00 (s, 2H, NH_2 exchanged with D_2O), 6.96–6.99 (dd, 2H, Ar-Hs, $^4J_{F\text{-}H}$ = 4.56 and 6.80 Hz), 7.07 (t, 2H, Ar-Hs, $^3J_{F\text{-}H}$ = 8.86 Hz); ^{13}C NMR (DMSO-d_6, 100 MHz): δ 24.96 , 25.32, 45.09, 48.51, 49.84, 75.26, 106.11, 115.78 ($^2J_{F\text{-}C}$ = 22.00 Hz), 116.31, 118.14 ($^3J_{F\text{-}C}$ = 7.00 Hz), 141.75, 145.92, 148.28, 156.68 ($^1J_{F\text{-}C}$ = 234.00 Hz), 162.86 (C=O); Anal. Calcd for $C_{19}H_{20}FN_5O$: C, 64.58; H, 5.70; N, 19.82. Found: C, 64.79; H, 5.88; N, 19.74.

*4.1.3.3. 6-Amino-5-[4-(4-chlorophenyl)piperazine-1-carbonyl]-2,3-dihydro-1H-pyrrolizine-7-carbonitrile(**4c**).* Yield: 85%; m.p.: 224–226 °C; IR (υ_{max}, cm^{-1}): 3445 and 3352 (NH_2), 3067 (CH-Ar.), 2967 (CH aliph.), 2207 (C≡N), 1645 (C=O); ^{1}H NMR (DMSO-d_6, 400 MHz): δ 2.36–2.39 (m, 2H, CH_2 of pyrrolizine), 2.86 (t, 2H, CH_2 of pyrrolizine, J = 7.32 Hz), 3.18 (s, br., 4H, CH_2 of piperazine), 3.55 (s, br., 4H, CH_2 of piperazine), 3.97 (t, 2H, CH_2 of pyrrolizine, J = 7.02 Hz), 5.00 (s, 2H, NH_2 exchanged with D_2O), 6.98 (d, 2H, Ar-Hs, J = 8.92 Hz), 7.25 (d, 2H, Ar-Hs, J = 8.84 Hz); ^{13}C NMR (DMSO-d_6, 100 MHz): δ 24.96 , 25.31, 44.91, 48.51, 48.79, 75.25, 106.08, 116.31, 117.71, 123.13, 129.13, 141.77, 145.94, 150.17, 162.86 (C=O); Anal. Calcd for $C_{19}H_{20}ClN_5O$: C, 61.70; H, 5.45; N, 18.94. Found: C, 61.94; H, 5.63; N, 19.25.

*4.1.3.4. 6-Amino-5-[4-(4-methoxyphenyl)piperazine-1-carbonyl]-2,3-dihydro-1H-pyrrolizine-7-carbonitrile(**4d**).* Yield: 79%; m.p.: 233–235 °C; IR (υ_{max}, cm^{-1}): 3449 and 3356 (NH_2), 3076 (CH-Ar.), 2951 (CH aliph.), 2203 (C≡N), 1645 (C=O); ^{1}H NMR (DMSO-d_6, 400 MHz): δ 2.34–2.41 (m, 2H, CH_2 of pyrrolizine), 2.86 (t, 2H, CH_2 of pyrrolizine, J = 7.30 Hz), 3.03 (s, br., 4H, CH_2 of piperazine), 3.56 (s, br., 4H, CH_2 of piperazine), 3.69 (s, 3H, OCH_3), 3.97 (t, 2H, CH_2 of pyrrolizine, J = 7.02 Hz), 4.98 (s, 2H, NH_2 exchanged with D_2O), 6.83 (d, 2H, Ar-Hs, J = 9.08 Hz), δ 6.92 (d, 2H, Ar-Hs, J = 8.96 Hz); ^{13}C NMR (DMSO-d_6, 100 MHz): 24.96 , 25.32, 45.23, 48.52, 50.54, 55.65 (OCH_3), 75.26, 106.15, 114.73, 116.31, 118.42, 141.71, 145.73, 145.88, 153.68, 162.83 (C=O); Anal. Calcd for $C_{20}H_{23}N_5O_2$: C, 65.73; H, 6.34; N, 19.16. Found: C, 66.02; H, 6.51; N, 19.40.

*4.1.3.5. 6-Amino-5-[4-(4-chlorobenzyl)piperazine-1-carbonyl]-2,3-dihydro-1H-pyrrolizine-7-carbonitrile(**4e**).* Yield: 85%; m.p.: 170–172 °C; IR (υ_{max}, cm^{-1}): 3395 and 3337 (NH_2), 3054 (CH-Ar.), 2936 (CH aliph.), 2214 (C≡N), 1643 (C=O); ^{1}H NMR (DMSO-d_6, 400 MHz): δ 2.38 (s, br., 6H, CH_2 of pyrrolizine and CH_2 of piperazine), 2.85 (t, 2H, CH_2 of pyrrolizine, J = 7.28 Hz), 3.42 (s, br., 4H, CH_2 of piperazine), 3.48 (s, 2H, benzylic CH_2), 3.95 (t, 2H, CH_2 of pyrrolizine, J = 7.00 Hz), 4.91 (s, 2H, NH_2 exchanged with D_2O), 7.34 (d, 2H, Ar-Hs, J = 8.28 Hz), 7.39 (d, 2H, Ar-Hs, J = 8.24 Hz); ^{13}C NMR (DMSO-d_6,

100 MHz): δ 24.94 , 25.32, 45.21, 48.51, 53.10, 61.45 (benzylic CH_2), 75.29, 106.20, 116.30, 128.65, 131.10, 131.97, 137.54, 141.70, 145.82, 162.82 (C=O); Anal. Calcd for $C_{20}H_{22}ClN_5O$: C, 62.58; H, 5.78; N, 18.24. Found: C, 62.79; H, 5.86; N, 18.43.

*4.1.3.6. 6-Amino-5-[4-(2,5-dimethoxybenzyl)piperazine-1-carbonyl]-2,3-dihydro-1H-pyrrolizine-7-carbonitrile(**4f**).* Yield: 76%; m.p.: 175–177 °C; IR (υ_{max}, cm^{-1}): 3414 and 3333 (NH_2), 3034 (CH-Ar.), 2947 (CH aliph.), 2210 (C≡N), 1645 (C=O); ^{1}H NMR (DMSO-d_6, 400 MHz): δ 2.35–2.41 (m, 6H, CH_2 of pyrrolizine & CH_2 of piperazine), 2.85 (t, 2H, CH_2 of pyrrolizine, J = 6.98 Hz), 3.44 (s, br., 4H, CH_2 of piperazine), 3.47 (s, 2H, benzylic CH_2), 3.71 (s, 3H, OCH_3), 3.72 (s, 3H, OCH_3), 3.95 (t, 2H, CH_2 of pyrrolizine, J = 6.58 Hz), 4.91 (s, 2H, NH_2 exchanged with D_2O), 6.80 (d, 1H, Ar-H, J = 8.36 Hz), 6.91 (d, 2H, Ar-Hs, J = 9.40 Hz); ^{13}C NMR (DMSO-d_6, 100 MHz): δ 24.94 , 25.32, 45.28, 48.50, 53.31, 55.73 (2 OCH_3), 56.37 (benzylic CH_2), 75.27, 106.22, 112.39, 112.58, 116.31, 127.26, 141.64, 145.77, 151.99, 153.49, 162.76 (C=O); Anal. Calcd for $C_{22}H_{27}N_5O_3$: C, 64.53; H, 6.65; N, 17.10. Found: C, 64.70; H, 6.79; N, 17.37.

*4.1.3.7. 6-Amino-N-(1-benzylpiperidin-4-yl)-7-cyano-2,3-dihydro-1H-pyrrolizine-5-carboxamide(**9**).* Yield: 77%; m.p.: 164–166 °C; IR (υ_{max}, cm^{-1}): 3406 and 3321 (NH_2), 3078 (CH-Ar.), 2947 (CH aliph.), 2210 (C≡N), 1643 (C=O); ^{1}H NMR (DMSO-d_6, 400 MHz): δ 1.53–1.56 (m, 2H, CH_2 of piperidine), 1.75–1.78 (m, 2H, CH_2 of piperidine), 2.01–2.06 (m, 2H, CH_2 of piperidine), 2.35–2.39 (m, 2H, CH_2 of pyrrolizine), 2.74–2.77 (m, 2H, CH_2 of piperidine), 2.85 (t, 2H, CH_2 of pyrrolizine, J = 7.40 Hz), 3.46 (s , 2H, benzylic CH_2), 3.67–3.71 (m, 1H, CH of piperidine), 4.13 (t, 2H, CH_2 of pyrrolizine, J = 7.04 Hz), 5.31 (s, 2H, NH_2 exchanged with D_2O), 6.89 (d, 1H, NH exchanged with D_2O, J = 7.60 Hz), 7.25–7.34 (m, 5H, Ar-Hs); ^{13}C NMR (DMSO-d_6, 100 MHz): δ 24.67 , 25.33, 32.08, 46.38, 49.52, 52.51, 62.60 (benzylic CH_2), 76.83, 107.64, 116.16, 127.30, 128.61, 129.14, 139.18, 144.57, 145.50, 160.99 (C=O); Anal. Calcd for $C_{21}H_{25}N_5O$: C, 69.40; H, 6.93; N, 19.27. Found: C, 69.23; H, 7.14; N, 19.59.

*4.1.4. General synthetic procedure for **5a–f** and **10***

A mixture of compound **4a–f or 9** (10 mmol) and 90% sulphuric acid (10 mL) was stirred for few minutes and left to stand for 48 h at room temperature. The reaction mixture poured over cold ammonia solution and left over night in a refrigerator. The product was filtered, washed with water, dried and recrystallized from ethanol to afford **5a–f** and **10**, respectively.

*4.1.4.1. 6-Amino-5-(4-phenylpiperazine-1-carbonyl)-2,3-dihydro-1H-pyrrolizine-7-carboxamide(**5a**).* Yield: 94%; m.p.: 277–279 °C; IR (υ_{max}, cm^{-1}): 3534, 3456, 3402 and 3325 (2 NH_2), 3082 (CH-Ar.), 2913 (CH aliph.), 1655 (2 C=O); ^{1}H NMR (DMSO-d_6, 400 MHz): δ 2.35 (s, br., 2H, CH_2 of pyrrolizine), 3.01 (s, br., 2H, CH_2 of pyrrolizine), 3.19 (s, br., 4H, CH_2 of piperazine), 3.56 (s, br., 4H, CH_2 of piperazine), 3.95 (s, br., 2H, CH_2 of pyrrolizine), 5.32 (s, 2H, NH_2 exchanged with D_2O), 6.54 (s, 2H, $CONH_2$, exchanged with D_2O), 6.81–6.83 (m, 1H, Ar-H), 6.98 (d, 2H, Ar-Hs, J = 6.88 Hz), 7.24 (s, br., 2H, Ar-Hs); ^{13}C NMR (DMSO-d_6, 100 MHz): δ 25.36 , 25.94, 45.31, 47.63, 49.11, 98.48, 106.02, 116.28, 119.63, 129.43, 141.58, 141.84, 151.46, 164.08 (C=O), 168.17 (C=O); Anal. Calcd for $C_{19}H_{23}N_5O_2$: C, 64.57; H, 6.56; N, 19.82. Found: C, 64.79; H, 6.63; N, 20.17.

*4.1.4.2. 6-Amino-5-[4-(4-fluorophenyl)piperazine-1-carbonyl]-2,3-dihydro-1H-pyrrolizine-7-carboxamide(**5b**).* Yield: 90%; m.p.: 280–282 °C; IR (υ_{max}, cm^{-1}): 3460, 3426, 3341 and 3306 (2 NH_2), 3039 (CH-Ar.), 2970 (CH aliph.), 1654 and 1643 (2 C=O); ^{1}H NMR (DMSO-d_6, 400 MHz): δ 2.31–2.39 (m, 2H, CH_2 of pyrrolizine), 3.00 (t, 2H, CH_2 of pyrrolizine, J = 7.30 Hz), 3.13 (t, 4H, CH_2 of piperazine, J = 4.40 Hz), 3.55 (t, 4H, CH_2 of piperazine, J = 4.72 Hz), 3.95 (t, 2H, CH_2 of pyrrolizine, J = 7.08 Hz), 5.32 (s, 2H, NH_2 exchanged with D_2O), 6.54 (s, 2H, $CONH_2$, exchanged with D_2O), 6.97–7.00 (dd, 2H, Ar-Hs, $^4J_{F\text{-}H}$ = 4.70 and 9.18 Hz), 7.08 (t, 2H, Ar-Hs, $^3J_{F\text{-}H}$ = 8.84 Hz); ^{13}C NMR (DMSO-d_6, 100 MHz): δ 25.34 , 25.94, 45.31, 47.63, 49.89, 98.44, 105.99, 115.77 ($^2J_{F\text{-}C}$ = 22.00 Hz), 118.12 ($^3J_{F\text{-}C}$ = 8.00 Hz), 141.67, 141.85, 148.34, 148.35, 156.66 ($^1J_{F\text{-}C}$ = 235.00 Hz), 164.08 (C=O), 168.19 (C=O); Anal. Calcd for $C_{19}H_{22}FN_5O_2$: C, 61.44; H, 5.97; N, 18.86. Found: C, 61.70; H, 6.12; N, 18.79.

*4.1.4.3. 6-Amino-5-[4-(4-chlorophenyl)piperazine-1-carbonyl]-2,3-dihydro-1H-pyrrolizine-7-carboxamide(**5c**).* Yield: 88%; m.p.: 276–278 °C; IR (υ_{max}, cm^{-1}): 3460, 3426, 3345 and 3310 (2 NH_2), 3036 (CH-Ar.), 2980 (CH aliph.), 1643 (2 C=O); ^{1}H NMR (DMSO-d_6, 400 MHz): δ 2.33–2.37 (m, 2H, CH_2 of pyrrolizine), 3.00 (t, 2H, CH_2 of pyrrolizine, J = 7.18 Hz), 3.20 (s, br., 4H, CH_2 of piperazine), 3.54 (s, br., 4H, CH_2 of piperazine), 3.95 (t, 2H, CH_2 of pyrrolizine, J = 6.94 Hz), 5.33 (s, 2H, NH_2 exchanged with D_2O), 6.54 (s, 2H, $CONH_2$, exchanged with D_2O), 6.99 (d, 2H, Ar-Hs, J = 8.88 Hz), 7.25 (d, 2H, Ar-Hs, J = 8.84 Hz); ^{13}C NMR (DMSO-d_6, 100 MHz): δ 25.36, 25.94, 45.14, 47.63, 48.84, 98.47, 105.99, 117.69, 123.07, 129.12, 141.61, 141.87, 150.25, 164.08 (C=O), 168.19 (C=O); Anal. Calcd for $C_{19}H_{22}ClN_5O_2$: C, 58.84; H, 5.72; N, 18.06. Found: C, 59.11; H, 5.86; N, 18.41.

*4.1.4.4. 6-Amino-5-[4-(4-methoxyphenyl)piperazine-1-carbonyl]-2,3-dihydro-1H-pyrrolizine-7-carboxamide(**5d**).* Yield: 92%; m.p.: 285–287 °C; IR (υ_{max}, cm^{-1}): 3395 and 3348 (2 NH_2), 3024 (CH-Ar.), 2970 (CH aliph.), 1654 and 1643 (2 C=O); ^{1}H NMR (DMSO-d_6, 400 MHz): δ 2.33–2.37 (m, 2H, CH_2 of pyrrolizine), 2.98–3.05 (m, 6H, CH_2 of pyrrolizine and CH_2 of piperazine), 3.54 (s, br., 4H, CH_2 of piperazine), 3.69 (s, 3H, OCH_3), 3.95 (t, 2H, CH_2 of pyrrolizine, J = 6.94 Hz), δ 5.34 (s, 2H, NH_2 exchanged with D_2O), 6.54 (s, 2H, $CONH_2$, exchanged with D_2O), 6.67 (d, 1H, Ar-H, J = 8.80 Hz), 6.84 (d, 1H, Ar-H, J = 9.04 Hz), 6.93 (d, 2H, Ar-Hs, J = 9.00 Hz); ^{13}C NMR (DMSO-d_6, 100 MHz): δ 25.36 , 25.94, 45.45, 47.63, 50.58, 55.64 (OCH_3), 98.49, 106.05, 114.73, 115.93, 118.38, 141.55, 145.80, 153.64, 164.05 (C=O), 168.17 (C=O), Anal. Calcd for $C_{20}H_{25}N_5O_3$: C, 62.65; H, 6.57; N, 18.26. Found: C, 62.93; H, 6.70; N, 18.62.

*4.1.4.5. 6-Amino-5-[4-(4-chlorobenzyl)piperazine-1-carbonyl]-2,3-dihydro-1H-pyrrolizine-7-carboxamide(**5e**).* Yield: 68%; m.p.: 190–192 °C; IR (υ_{max}, cm^{-1}): 3483, 3441 and 3310 (2 NH_2), 3075 (CH-Ar.), 2981 (CH aliph.), 1654 and 1643 (2 C=O); ^{1}H NMR (DMSO-d_6, 400 MHz): δ 2.32–2.39 (m, 6H, CH_2 of pyrrolizine and CH_2 of piperazine), 2.99 (t, 2H, CH_2 of pyrrolizine, J = 6.86 Hz), 3.41 (s, br., 4H, CH_2 of piperazine), 3.49 (s, 2H, benzylic CH_2), 3.92 (t, 2H, CH_2 of pyrrolizine, J = 6.64 Hz), 5.24 (s, 2H, NH_2 exchanged with D_2O), 6.52 (s, 2H, $CONH_2$, exchanged with D_2O), 7.34 (d, 2H, Ar-Hs, J = 8.00 Hz), 7.39 (d, 2H, Ar-Hs, J = 8.04 Hz); ^{13}C NMR (DMSO-d_6, 100 MHz): δ 25.36 , 25.92, 45.40, 47.61, 53.20, 61.52 (benzylic CH_2), 98.51, 106.04, 128.65, 131.10, 131.95, 137.61, 141.45, 141.77, 163.97 (C=O), 168.13 (C=O), Anal. Calcd for $C_{20}H_{24}ClN_5O_2$: C, 59.77; H, 6.02; N, 17.43. Found: C, 59.89; H, 6.17; N, 17.56.

*4.1.4.6. 6-Amino-5-[4-(2,5-dimethoxybenzyl)piperazine-1-carbonyl]-2,3-dihydro-1H-pyrrolizine-7-carboxamide(**5f**).* Yield: 68%; m.p.: 185–187 °C; IR (υ_{max}, cm^{-1}): 3464, 3418, 3345 and 3310 (2 NH_2), 3054 (CH-Ar.), 2985 (CH aliph.), 1654 and 1643 (2 C=O); ^{1}H NMR (DMSO-d_6, 400 MHz): δ 2.32–2.36 (m, 2H, CH_2 of pyrrolizine), 2.43 (s, br., 4H, CH_2 of piperazine), 2.98 (t, 2H, CH_2 of pyrrolizine, J = 7.22 Hz), 3.43 (s, br., 4H, CH_2 of piperazine), 3.47 (s, 2H, benzylic CH_2), 3.70 (s, 3H, OCH_3), 3.72 (s, 3H, OCH_3), 3.92 (t, 2H, CH_2 of pyrrolizine, J = 7.00 Hz), 5.23 (s, 2H, NH_2 exchanged with D_2O), 6.52 (s, 2H, $CONH_2$, exchanged with D_2O), 6.80 (d, 1H, Ar-H, J = 8.80 Hz), 6.90–7.12 (m, 2H, Ar-Hs);^{13}C NMR (DMSO-d_6, 100 MHz): δ 25.36, 25.92, 45.45, 47.61, 53.41, 55.73, 55.79 (2OCH_3), 56.37 (benzylic CH_2), 98.49, 106.05, 112.40, 112.58, 116.29, 127.31, 141.41,

141.70, 151.99, 153.50, 163.91 (C=O), 168.14 (C=O), Anal. Calcd for $C_{22}H_{29}N_5O_4$: C, 61.81; H, 6.84; N, 16.38. Found: C, 62.12; H, 6.97; N, 16.57.

*4.1.4.7. 6-Amino-N^5-(1-benzylpiperidin-4-yl)-2,3-dihydro-1H-pyrrolizine-5,7-dicarboxamide(**10**).* Yield: 65%; m.p.: 189–191 °C; IR (υ_{max}, cm^{-1}): 3441, 3399 and 3302 (2 NH_2 and NH), 3028 (CH-Ar.), 2946 (CH aliph.), 1635 (2 C=O); ^{1}H NMR (DMSO-d_6, 400 MHz): δ 1.53–1.56 (m, 2H, CH_2 of piperidine), 1.77–1.79 (m, 2H, CH_2 of piperidine), 2.02–2.09 (m, 2H, CH_2 of piperidine), 2.32–2.36 (m, 2H, CH_2 of pyrrolizine), 2.74–2.77 (m, 2H, CH_2 of piperidine), 2.97 (t, 2H, CH_2 of pyrrolizine, J = 7.26 Hz), 3.46 (s , 2H, benzylic CH_2), 3.71 (m, 1H, CH of piperidine), 4.08 (t, 2H, CH_2 of pyrrolizine, J = 6.94 Hz), 5.56 (s, 2H, NH_2 exchanged with D_2O), 6.60 (d, 3H, NH_2 and NH exchanged with D_2O, J = 7.52 Hz), 7.25–7.34 (m, 5H, Ar-Hs); ^{13}C NMR (DMSO-d_6, 100 MHz): δ 25.39, 25.62, 32.23, 46.20, 48.46, 52.55, 62.62 (benzylic CH_2), 99.87, 107.26, 117.30, 127.30, 128.61, 129.16, 141.09, 143.99, 161.51 (C=O), 167.97 (C=O), Anal. Calcd for $C_{21}H_{27}N_5O_2$: C, 66.12; H, 7.13; N, 18.36. Found: C, 66.03; H, 7.40; N, 18.62.

*4.1.5. General synthetic procedure for **6a–f** and **11***

Compounds **4a–g** or **9** (3.8 mmol) were heated under reflux with 90% formic acid (15 mL) for 4 h. After cooling, 10% sodium hydroxide was added slowly until the mixture was just alkaline to litmus. The formed precipitate was filtered, washed with water, dried and recrystallized from ethanol to obtain compounds **6a–f** and **11**, respectively.

*4.1.5.1. 9-(4-Phenylpiperazine-1-carbonyl)-6,7-dihydro-3H-pyrimido[5,4-a]pyrrolizin-4(5H)-one(**6a**).* Yield: 86%; m.p.: 264–266 °C; IR (υ_{max}, cm^{-1}): 3414 (NH), 3024 (CH-Ar.), 2913 (CH aliph.), 1686 (2 C=O); ^{1}H NMR (DMSO-d_6, 400 MHz): δ 2.51 (s, br., 2H, CH_2 of pyrrolizine), 3.10 (t, 2H, CH_2 of pyrrolizine, J = 6.98 Hz), 3.23 (s, br., 4H, CH_2 of piperazine), 3.76 (s, br., 4H, CH_2 of piperazine), 4.27 (t, 2H, CH_2 of pyrrolizine, J = 6.92 Hz), 6.81 (t , 1H, Ar-H, J = 7.06 Hz), 6.98 (d, 2H, Ar-Hs, J = 7.96 Hz), 7.24 (t, 2H, Ar-Hs, J = 7.56 Hz), 7.74 (s, 1H, CH of pyrimidinone), 11.41 (s, 1H, NH exchanged with D_2O); ^{13}C NMR (DMSO-d_6, 100 MHz): δ 25.51, 26.01, 48.58, 49.25, 102.58, 112.41, 116.36, 119.74, 129.45, 138.70, 139.98, 144.09, 151.39, 159.01 (C=O), 161.19 (C=O); Anal. Calcd for $C_{20}H_{21}N_5O_2$: C, 66.10; H, 5.82; N, 19.27. Found: C, 66.37; H, 6.11; N, 19.43.

*4.1.5.2. 9-[4-(4-Fluorophenyl)piperazine-1-carbonyl]-6,7-dihydro-3H-pyrimido[5,4-a]pyrrolizin-4(5H)-one(**6b**).* Yield: 78%; m.p.: 274–276 °C; IR (υ_{max}, cm^{-1}): 3352 (NH), 3055 (CH-Ar.), 2959 (CH aliph.), 1686 (2 C=O); ^{1}H NMR (DMSO-d_6, 400 MHz): δ 2.51 (s, br., 2H, CH_2 of pyrrolizine), 3.10 (s, br., 2H, CH_2 of pyrrolizine), 3.17 (s, br., 4H, CH_2 of piperazine), 3.76 (s, br., 4H, CH_2 of piperazine), 4.27 (s, br., 2H, CH_2 of pyrrolizine), 7.00–7.12 (dd, 2H, Ar-Hs, $^4J_{F\text{-}H}$ = 4.72 and 8.21 Hz), 7.07 (t, 2H, Ar-Hs, $^3J_{F\text{-}H}$ = 8.86 Hz), 7.73 (s, 1H, CH of pyrimidinone), 11.41 (s, 1H, NH exchanged with D_2O); ^{13}C NMR (DMSO-d_6, 100 MHz): δ 25.51, 26.02, 48.59 50.25, 102.64, 112.41, 115.80 ($^2J_{F\text{-}C}$ = 21.00 Hz), 118.20 ($^3J_{F\text{-}C}$ = 7.00 Hz), 138.63, 139.99, 144.13, 148.32, 157.15 ($^1J_{F\text{-}C}$ = 230.00 Hz), 158.93 (C=O), 161.14 (C=O); Anal. Calcd for $C_{20}H_{20}FN_5O_2$: C, 62.98; H, 5.29; N, 18.36. Found: C, 63.11; H, 5.45; N, 18.59.

*4.1.5.3. 9-[4-(4-Chlorophenyl)piperazine-1-carbonyl]-6,7-dihydro-3H-pyrimido[5,4-a]pyrrolizin-4(5H)-one(**6c**).* Yield: 72%; m.p.: 276–278 °C; IR (υ_{max}, cm^{-1}): 3422 (NH), 3075 (CH-Ar.), 2967 (CH aliph.), 1674 (2 C=O); ^{1}H NMR (DMSO-d_6, 400 MHz): δ 2.51 (s, br., 2H, CH_2 of pyrrolizine), 3.10 (t, 2H, CH_2 of pyrrolizine, J = 7.34 Hz), 3.24 (s, br., 4H, CH_2 of piperazine), 3.75 (s, br., 4H, CH_2 of piperazine), 4.27 (t, 2H, CH_2 of pyrrolizine, J = 7.16 Hz), 6.99 (d, 2H, Ar-Hs, J = 8.92 Hz), 7.26 (d, 2H, Ar-Hs, J = 8.88 Hz), 7.73 (s, 1H, CH of pyrimidinone), 11.39 (s, 1H, NH exchanged with D_2O); ^{13}C NMR (DMSO-d_6, 100 MHz): δ 25.53, 26.03, 48.61, 49.25, 102.64, 112.39, 117.75, 123.17, 129.14, 138.68, 144.15, 150.21, 158.93 (C=O), 161.18 (C=O); Anal. Calcd for $C_{20}H_{20}ClN_5O_2$: C, 60.38; H, 5.07; N, 17.60. Found: C, 60.56; H, 5.30; N, 17.29.

*4.1.5.4. 9-[4-(4-Methoxyphenyl)piperazine-1-carbonyl]-6,7-dihydro-3H-pyrimido[5,4-a]pyrrolizin-4(5H)-one(**6d**).* Yield: 71%; m.p.: 281–283 °C; IR (υ_{max}, cm^{-1}): 3395 (NH), 3063 (CH-Ar.), 2920 (CH aliph.), 1670 (2 C=O); ^{1}H NMR (DMSO-d_6, 400 MHz): δ 2.51 (s, br., 2H, CH_2 of pyrrolizine), 3.10 (s, br., 6H, CH_2 of pyrrolizine and CH_2 of piperazine), 3.70 (s, 3H, OCH_3), 3.75 (s, br., 4H, CH_2 of piperazine), 4.27 (t, 2H, CH_2 of pyrrolizine, J = 7.16 Hz), 6.84 (d, 2H, Ar-Hs, J = 9.00 Hz), 6.94 (d, 2H, Ar-Hs, J = 9.00 Hz), 7.73 (s, 1H, CH of pyrimidinone), 11.40 (s, 1H, NH exchanged with D_2O); ^{13}C NMR (DMSO-d_6, 100 MHz): δ 25.51, 26.03, 48.58, 50.25, 55.65 (OCH_3), 102.63, 112.46, 114.74, 118.46, 138.57, 139.94, 144.09, 145.77, 153.70, 158.94 (C=O), 161.12 (C=O); Anal. Calcd for $C_{21}H_{23}N_5O_3$: C, 64.11; H, 5.89; N, 17.80. Found: C, 64.38; H, 6.12; N, 18.14.

*4.1.5.5. 9-[4-(4-Chlorobenzyl)piperazine-1-carbonyl]-6,7-dihydro-3H-pyrimido[5,4-a]pyrrolizin-4(5H)-one(**6e**).* Yield: 77%; m.p.: 183–185 °C; IR (υ_{max}, cm^{-1}): 3445 (NH), 3048 (CH-Ar.), 2916 (CH aliph.), 1670 (2 C=O); ^{1}H NMR (DMSO-d_6, 400 MHz): δ 2.45 (s, br., 6H, CH_2 of pyrrolizine and CH_2 of piperazine), 3.08 (t, 2H, CH_2 of pyrrolizine, J = 6.62 Hz), 3.51 (s, 2H, benzylic CH_2), 3.61 (s, br., 4H, CH_2 of piperazine), 4.24 (t, 2H, CH_2 of pyrrolizine, J = 6.48 Hz), 7.36 (d, 2H, Ar-Hs, J = 7.52 Hz), 7.4 (d, 2H, Ar-Hs, J = 7.8 Hz), 7.70 (s, 1H, CH of pyrimidinone), 11.38 (s, 1H, NH exchanged with D_2O); ^{13}C NMR (DMSO-d_6, 100 MHz): δ 25.49, 26.01, 48.56, 53.37, 61.42 (benzylic CH_2), 102.59, 112.52, 128.65, 131.08 131.96, 137.58, 138.45, 139.82, 143.96, 158.93 (C=O), 161.10 (C=O); Anal. Calcd for $C_{21}H_{22}ClN_5O_2$: C, 61.24; H, 5.38; N, 17.00. Found: C, 61.53; H, 5.51; N, 16.89.

*4.1.5.6. 9-[4-(2,5-Dimethyoxybenzyl)piperazine-1-carbonyl]-6,7-dihydro-3H-pyrimido[5,4-a]pyrrolizin-4(5H)-one(**6f**).* Yield: 66%; m.p.: 189–191 °C; IR (υ_{max}, cm^{-1}): 3395 (NH), 3067 (CH-Ar.), 2909 (CH aliph.), 1670 (2 C=O); ^{1}H NMR (DMSO-d_6, 400 MHz): δ 2.45 (s, br., 6H, CH_2 of pyrrolizine and CH_2 of piperazine), 3.08 (s, br., 2H, CH_2 of pyrrolizine), 3.49 (s, 2H, benzylic CH_2), 3.62 (s, br., 4H, CH_2 of piperazine), 3.71 (s, 3H, OCH_3), 3.73 (s, 3H, OCH_3), 4.24 (s, br., 2H, CH_2 of pyrrolizine), 6.80 (d, 1H, Ar-H, J = 8.36 Hz), 6.90–6.94 (m, 2H, Ar-Hs), 7.70 (s, 1H, CH of pyrimidinone), 11.37 (s, 1H, NH exchanged with D_2O); ^{13}C NMR (DMSO-d_6, 100 MHz): δ 25.49, 26.02, 48.53, 53.37, 55.74 (2 OCH_3), 56.35 (benzylic CH_2), 102.58, 112.37, 112.50, 112.57, 116.28, 127.28, 138.38 139.79, 143.93, 151.97, 153.51, 158.94 (C=O), 161.05 (C=O); Anal. Calcd for $C_{23}H_{27}N_5O_4$: C, 63.14; H, 6.22; N, 16.01. Found: C, 63.38; H, 6.48; N, 15.89.

*4.1.5.7. N-(1-Benzylpiperidin-4-yl)-4-oxo-4,5,6,7-tetrahydro-3H-pyrimido[5,4-a]pyrrolizine-9-carboxamide(**11**).* Yield: 65%; m.p.: 196–198 °C; IR (υ_{max}, cm^{-1}): 3445 and 3240 (2 NH), 3009 (CH-Ar.), 2974 (CH aliph.), 1686 (2 C=O); ^{1}H NMR (DMSO-d_6, 400 MHz): δ 1.50 (s, br., 2H, CH_2 of piperidine), 1.89 (s, br., 2H, CH_2 of piperidine), 2.16 (s, br., 2H, CH_2 of piperidine), 2.72 (s, br., 2H, CH_2 of pyrrolizine), 3.07 (s, br., 4H, CH_2 of piperidine and CH_2 of pyrrolizine), 3.40 (s , 2H, benzylic CH_2), 3.83 (s, br., 1H, CH of piperidine), 4.41 (s, br., 2H, CH_2 of pyrrolizine), 7.33 (s, br., 5H, Ar-Hs), 7.86 (s, 1H, CH of pyrimidinone), 8.12 (s, 1H, NH exchanged with D_2O), 11.61 (s, 1H, NH exchanged with D_2O); ^{13}C NMR (DMSO-d_6, 100 MHz): δ 24.97, 26.19, 32.52, 45.63, 49.37, 51.96, 62.58 (benzylic CH_2), 103.18, 111.87, 127.31, 128.62, 129.17, 138.36, 139.06, 145.44, 158.52 (C=O), 160.05 (C=O); Anal. Calcd for $C_{22}H_{25}N_5O_2$: C, 67.50; H, 6.44; N, 17.89. Found: C, 67.34; H, 6.72; N, 18.21.

4.2. Cholinesterase inhibitory assay

*h*AChE and *h*BChE inhibitory potencies of the compounds were measured by slightly modifying the colorimetric Ellman's method as described previously [28,29]. Acetylthiocholine iodide (AChI) and butyrylthiocholine iodide (BChI) were used as substrates of the enzymatic reaction. Additionally, 5,5-dithiobis(2-nitro-benzoic acid) (DTNB) was used as common substrate for the determination of the AChE and BChE activities. Briefly, 1 mL of Tris/HCl buffer (1.0 M, pH = 8) and 10 mL of sample solution at different concentrations were dissolved in ultra-pure water. Then, 50 mL *h*AChE or *h*BChE solution was mixed and incubated at room temperature for 10 min. After incubation period, 50 mL of DTNB (0.5 mM) was added. Then, the reaction was allowed to start by the addition of 50 mL of AChI (10 mM) or BChI. The breakdown of these substrates was monitored spectrophotometrically by yellow color formation of 5-thio-2-nitrobenzoate anion as the result of the reaction of DTNB with thiocholine from hydrolysis of AChI or BChI with absorption at a wavelength of 412 nm. Ki values were calculated from Lineweaver – Burk curves.

4.3. Kinetic study

Kinetic characterization of AChE was carried out experimentally using Ellman's method [28,29] with three different concentrations of the inhibitor (0.00025, 0.00051, 0.00063 nM) in addition to a parallel experiment that is carried out in absence of inhibitor. Lineweaver-Burk reciprocal plots were constructed by plotting 1/velocity against 1/[Substrate]. Then the results were analyzed using Microsoft Office Excel 2013.

4.4. Self-induced amyloid-beta aggregation

Inhibition of $A\beta_{1-42}$ aggregation assay was performed for all the synthesized compounds at 5 different concentrations (0.01, 0.1, 1.0, 10 and 100 μM) using Oligomeric Amyloid-β (o-Aβ) ELISA Kit (BEK-2215-1P/2P) obtained from Biosensis®. O-Aβ was purchased from Sigma Aldrich®. The assay was carried out according the reported sensitive and high-throughput enzyme-linked immunosorbent assay (ELISA) method [30]. Optical density (OD_{450}) values were measured on a plate reader at wavelength 450 nm. A standard curve plotted with the o-Aβ standard concentration on the x-axis and the OD_{450} on the y-axis. Finally, o-Aβ concentration of the samples interpolated from the standard curve.

4.5. SH-SY5Y neuroblastoma cell toxicity and THLE2 hepatoma cell toxicity

The cytotoxicity effect of test compounds **10** and **11** on the human neuroblastoma SH-SY5Y cells and THLE2 hepatoma cells were evaluated by MTT assay [31] using IN VITRO TOXICOLOGY ASSAY KIT MTT BASED (TOX-1), Sigma Aldrich®. SH-SY5Y cells (ATCC, Manassas, VA, USA), were cultured using Eagle's minimum essential medium (EMEM) with 4.5 g/L glucose, supplemented with 10% fetal bovine serum FBS, 100U/mL penicillin, and 100 μg/mL streptomycin in 5% CO_2 at 37 °C. THLE-2 cells (ATCC, Manassas, VA, USA), were cultured in Bronchial Epithelial Basal Medium (BEBM) instead EMEM supplemented with 1% fetal calf serum (FCS) and antibiotics (50 mg/ml each of penicillin, streptomycin and gentamicin). For cell viability assay, plate the cells into 96-well plates at a seeding density 10,000 cells/well then incubated cells were exposed to increasing concentrations (from 0.01 to 100 μM) of the test compounds **10** and **11** for 24 h before the MTT assay. After the incubation period, 20 mL of MTT at 37 °C was added for 4 hr, then remove cultures from incubator and dissolve the resulting formazan crystals by adding 200 mL of DMSO. Spectrophotometrically absorbance measured at wavelength of 570 nm. Results are expressed as the mean ± SD of three independent experiments.

4.6. In vivo behavioral studies

Adult Swiss Albino mice (8–10 weeks old, weight 25–30 g) were supplied from Vacsera. Mice were maintained in animal house with well-ventilated cages with free access to standard forage. Animals adapted for one week in a room controlled for temperature (25 ± 2 °C), humidity (60 ± 10%), and lighting (12 h light–dark cycle). Food and water were provided ad libitum throughout the experiment. Mice were housed in well ventilated opaque propylene cages with free access to standard forage. The mice were divided into five groups: **i)** control or vehicle (normal saline) group, **ii)** model or scopolamine group (0.5 mg/kg, i.p.), **iii)** scopolamine plus donepezil (5 mg/kg, p.o), **iv)** scopolamine plus compound **10** (5 mg/kg, p.o) and **v)** scopolamine plus compound **11** (5.2 mg/kg, p.o). The dose of the compounds was fixed on the basis of equimolar doses compared with donepezil. Donepezil and test compounds were administered once daily for 7 seven days to the respective group of animals. Scopolamine-group of rats was given vehicle only. All group animals except vehicle were administered with scopolamine on the seventh day to induce amnesia. Donepezil and test compounds were administered 30 min before memory impairment induction by scopolamine.

In Y-maze test [32], Y-maze composed of three equally spaced horizontal arms (120°, 45 cm long and 16 cm high). Each mouse was placed into one of the three arms and allowed to move freely between the arms of the maze. The sequence of arm entries and number of arm entries were recorded. The spontaneous alternation is a measure of the memory performace and calculated from the following equation: % alternation = (number of alternations/(total arm entries) − 2) × 100.

Step-through passive avoidance test [33] was carried in an apparatus which divided into two distinct chambers. The illuminated chamber which is free from electric stimuli was connected to a dark compartment with electrifiable grid floor. Both chambers were separated by a sliding door. Then, the mice underwent two separate trials: a training trial and a test trial. The training trial was performed by placing each mouse in the illuminated chamber and allowed to get familiar with it. Next, the sliding door is opened to allow entering in the dark compartment. When the animal stepped completely in the dark chamber, the door was closed and the animal received an electric foot shock ((24 V, 0.5 mA) for 2 s. Latency time to enter the dark compartment was recorded which measure the working memory. Twenty-four hours after the training trial, a test trial was performed but no electric foot shock applied.

4.7. Molecular docking studies

Docking studies aims to identify molecular features that are responsible for specific biological recognition, or prediction of structural modifications that improve potency. X-ray crystal structure of acetylcholineterase in complex with donepezil (Aricept®, E2020) was downloaded from https://www.rcsb.org/structure/4ey7 (PDB ID: 4ey7). All molecular modeling calculations and docking studies were carried out using Molecular Operating Environment (MOE 10. 2008) software [34] provided by chemical computing group, Canada. First, water molecules were deleted except the one involved in a water-mediated hydrogen bond with donepezil, protons and partial charges were added to protein structure. To ensure the accuracy of the docking protocol, validation was performed by re-docking the co-crystallized ligand (donepezil) into acetylcholinesterase active site. The docking validation results showed a near perfect alignment with the original ligand with rmsd of 0.5805 and score of-13.0985 Kcal/mol, displaying the same binding interactions. Target compounds were protonated, energy minimized by Merk Molecular Force Field (MMFF94X) to a gradient 0.05. Docking of the most stable conformers was done with MOEDOCK using Triangle Matcher Replacement and London dG scoring function.

Funding

This research did not receive any specific grant from funding agencies in the public, commercial, or not-for-profit sectors.

References

[1] A.s. Association, Alzheimer's disease facts and figures, Alzheimer's Dement. 12 (2016) (2016) 459–509, https://doi.org/10.1016/j.jalz.2016.03.001.
[2] J. Mendiola-Precoma, L.C. Berumen, K. Padilla, G. Garcia-Alcocer, Therapies for prevention and treatment of Alzheimer's disease, BioMed. Res. Int. 2016 (2016) 1–17, https://doi.org/10.1155/2016/2589276.
[3] M. Xu, Y. Peng, L. Zhu, S. Wang, J. Ji, K.P. Rakesh, Triazole derivatives as inhibitors of Alzheimer's disease: current developments and structure-activity relationships, Eur. J. Med. Chem. 180 (2019) 656–672, https://doi.org/10.1016/j.ejmech.2019.07.059.
[4] Alzheimer's Association, Alzheimer's disease facts and figures, Alzheimer's Dement. 11 (2015) (2015) 332–384.
[5] B. Kumar, V. Kumar, V. Prashar, S. Saini, A.R. Dwivedi, B. Bajaj, D. Mehta, J. Parkash, V. Kumar, Dipropargyl substituted diphenylpyrimidines as dual inhibitors of monoamine oxidase and acetylcholinesterase, Eur. J. Med. Chem. 177 (2019) 221–234, https://doi.org/10.1016/j.ejmech.2019.05.039.
[6] G. Šimić, M. Babić Leko, S. Wray, C. Harrington, I. Delalle, N. Jovanov-Milošević, D. Bažadona, L. Buée, R. de Silva, G. Di Giovanni, C. Wischik, P.R. Hof, Tau protein hyperphosphorylation and aggregation in Alzheimer's disease and other tauotherapies, and possible neuroprotective strategies, Biomolecules 6 (2016), https://doi.org/10.3390/biom6010006.
[7] J. Haam, J.L. Yakel, Cholinergic modulation of the hippocampal region and memory function, J. Neurochem. 142 (2017) 111–121.
[8] W.J. Deardorff, E. Feen, G.T. Grossberg, The use of cholinesterase inhibitors across all stages of Alzheimer's disease, Drug Aging 32 (2017) 537–547, https://doi.org/10.1007/s40266-015-0273-x.
[9] T. Umar, N. Hoda, Alzheimer's disease: a systemic review of substantial therapeutic targets and the leading multi-functional molecules, Curr. Top Med. Chem. 17 (2017) 3370–3389, https://doi.org/10.2174/1568026618666180112161 0.
[10] D. Galimberti, E. Scarpini, Old and new acetylcholinesterase inhibitors for Alzheimer's disease, Expert. Opin. Investig. Drugs 25 (2016) 1181–1187, https://doi.org/10.1080/13543784.2016.1216972.
[11] X. Chen, L. Fang, J. Liu, C.-G. Zhan, Reaction pathway and free energy profiles for butyrylcholinesterase-catalyzed hydrolysis of acetylthiocholine, Biochemistry 51 (2012) 1297–1305, https://doi.org/10.1021/bi201786s.
[12] P. Srivastava, P.N. Tripathi, P. Sharma, S.K. Shrivastava, Design, synthesis, and evaluation of novel N-(4-phenoxybenzyl)aniline derivatives targeting acetylcholinesterase, β-amyloid aggregation and oxidative stress to treat Alzheimer's disease, Bioorg. Med. Chem. 27 (2019) 3650–3662, https://doi.org/10.1016/j.bmc.2019.07.001.
[13] J. Godyn, J. Jonczyk, D. Panek, B. Malawska, Theraputic strategies for Alzheimer's disease in clinical trials, Pharmacol. Rep. 68 (2016) 127–138, https://doi.org/10.1016/j.pharep.2015.07.006.
[14] J. Lalut, G. Santoni, D. Karila, C. Lecoutey, A. Davis, F. Nachon, I. Silman, J. Sussman, M. Weik, T. Maurice, P. Dallemagne, C. Rochais, Novel multitarget-directed ligands targeting acetylcholinesterase and s1 receptors as lead compounds for treatment of Alzheimer's disease: synthesis, evaluation, and structural characterization of their complexes with acetylcholinesterase, Eur. J. Med. Chem. 162 (2019) 234–248, https://doi.org/10.1016/j.ejmech.2018.10.064.
[15] A. Kumar, A. Singh, Ekavali, A review on Alzheimer's disease pathophysiology and its management: an update, Pharmacol. Rep. 67 (2015) 195–203, https://doi.org/10.1016/j.pharep.2014.09.004.
[16] A. Kimura, S. Hata, T. Suzuki, Alternative selection of b-site APP-cleaving enzyme 1 (BACE1) cleavage sites in amyloid b-protein precursor (APP) harboring protective and pathogenic mutations within the Ab sequence, J. Biol. Chem. 291 (2016) 24041–24053, https://doi.org/10.1074/jbc.M116.744722.
[17] R.J. Andrew, K.A. Kellett, G. Thinakaran, N.M. Hooper, A Greek tragedy: the growing complexity of Alzheimer amyloid precursor protein proteolysis, J. Biol. Chem. 291 (2016) 19235–19244, https://doi.org/10.1074/jbc.R116.746032.
[18] R.A. Marr, D.M. Hafez, amyloid-beta and Alzheimer's disease: the role of neprilysin-2 in amyloid-beta clearance, Aging Neurosci. 6 (2014) 187–193, https://doi.org/10.3389/fnagi.2014.00187.
[19] M.A. Maia, E. Sousa, BACE-1 and γ-Secretase as Therapeutic Targets for Alzheimer's Disease, Pharmaceuticals 12 (2019) 41, https://doi.org/10.3390/ph12010041.
[20] H. Benamar, L. Tomassini, A. Venditti, A. Marouf, M. Bennaceur, M. Nicoletti, Pyrrolizidine alkaloids from Solenanthus lanatus DC. with acetylcholinesterase inhibitory activity, Nat. Prod. Res. 30 (2016) 2567–2574, https://doi.org/10.1080/14786419.2015.1131984.
[21] Y. Kia, H. Osman, R.S. Kumar, V. Murugaiyah, A. Basiri, S. Perumal, H.A. Wahab, C.S. Bing, Synthesis and discovery of novel piperidone-grafted mono- and bis-spirooxindole-hexahydropyrrolizines as potent cholinesterase inhibitors, Bioorg. Med. Chem. 21 (2013) 1696–1707, https://doi.org/10.1016/j.bmc.2013.01.066.
[22] Y. Kia, H. Osman, R.S. Kumar, V. Murugaiyah, A. Basiri, S. Perumal, I.A. Razak, A facile chemo-, regio- and stereoselective synthesis and cholinesterase inhibitory activity of spirooxindole–pyrrolizine–piperidine hybrids, Bioorg. Med. Chem. 23 (2013) 2979–2983, https://doi.org/10.1016/j.bmcl.2013.03.027.
[23] J. Zhang, D. Zhu, R. Sheng, H. Wu, Y. Hu, F. Wang, T. Cai, B. Yang, Q. He, BZYX, a novel acetylcholinesterase inhibitor, significantly improved chemicals-induced learning and memory impairments on rodents and protected PC12 cells from apoptosis induced by hydrogen peroxide, Eur. J. Pharmacol. 613 (2009) 1–9, https://doi.org/10.1016/j.ejphar.2009.03.054.
[24] A. Etienne, Y. Correia, Derivatives of 2-pyrrolidone, Bull. Soc. Chem. 10 (1969) 3704–3712.
[25] M.Y. Ebeid, I. Bitter, Condensed pyrimidine-III. Synthesis and structure assignment of pyrido[1,2-c]pyrimidines, Egypt, J. Pharm. Sci. 19 (1978) 349–353.
[26] J. Bourdais, Alkylation of piperazines in *N*, *N*-dimethylformamide, Bull. Soc. Chim., Fr. 8 (1968) 3246.
[27] C. Zhang, C. Tan, X. Zu, X. Zhai, F. Liu, B. Chu, X. Ma, Y. Chen, P. Gong, Y. Jiang, Exploration of (S)-3-aminopyrrolidine as a potentially interesting scaffold for discovery of novel Abl and PI3K dual inhibitors, J. Eur. Med. Chem. 46 (2011) 1404–1414 DOI: 0.1016/j.ejmech.2011.01.020.
[28] C. Yamali, H.I. Gul, A. Ece, P. Taslimi, I. Gulcin, Synthesis, molecular modeling, and biological evaluation of 4-[5-aryl-3-(thiophen-2-yl)-4,5-dihydro-1H-pyrazol-1-yl] benzenesulfonamides toward acetylcholinesterase, carbonic anhydrase I and II enzymes, Chem. Biol. Drug Des. 91 (2018) 854–866, https://doi.org/10.1111/cbdd.13149.
[29] S. Burmaoglu, A.O. Yilmaz, P. Taslimi, O. Algul, D. Kilic, I. Gulcin, Synthesis and biological evaluation of phloroglucinol derivatives possessing alpha-glycosidase, acetylcholinesterase, butyrylcholinesterase, carbonic anhydrase inhibitory activity, Arch. Pharm. 351 (2018) 1–12, https://doi.org/10.1002/ardp.201700314.
[30] K.A. Bruggink, W. Jongbloed, E.A. Biemans, R. Veerhuis, J.A. Claassen, H.B. Kuiperij, M.M. Verbeek, Amyloid-β oligomer detection by ELISA in cerebrospinal fluid and brain tissue, Anal. Biochem. 433 (2013) 112–120, https://doi.org/10.1016/j.ab.2012.09.014.
[31] X. Li, H. Wang, Z. Lu, X. Zheng, W. Ni, J. Zhu, Y. Fu, F. Lian, N. Zhang, J. Li, H. Zhang, F. Mao, Development of multifunctional pyrimidinylthiourea derivatives as potential anti-Alzheimer agents, J. Med. Chem. 59 (2016) 8326–8344, https://doi.org/10.1021/acs.jmedchem.6b00636.
[32] K. Dam, M. Fuchtemeier, T.D. Farr, P. Boehm-Sturm, M. Foddis, U. Dirnagl, O. Malysheva, M.A. Caudill, N.M. Jadavji, Increased homocysteine levels impair reference memory and reduce cortical levels of acetylcholine in a mouse model of vascular cognitive impairment, Behav. Brain Res. 321 (2017) 201–208, https://doi.org/10.1016/j.bbr.2016.12.041.
[33] Z. Bohdanecký, M. Jarvik, Impairment of one-trial passive avoidance learning in mice by scopolamine, scopolamine methylbromide, and physostigmine, Int. J. Neuropharmacol. 6 (1967) 217–222, https://doi.org/10.1016/S0163-1047(88)90938-7.
[34] MOE. Chemical computing Group, Inc., Montereal, < https://www.chemcomp.com/ > .
[35] B. Kuzu, M. Tan, P. Taslimi, I. Gülçin, M. Taşpınar, N. Menges, Mono-or Di-substituted imidazole derivatives for inhibiton of acetylcholine and butyrylcholine esterases, Bioorg. Chem. 86 (2019) 187–196, https://doi.org/10.1016/j.bioorg.2019.01.044.